High-P_T Physics: from the Tevatron to the LHC

Tommaso Dorigo

Dipartimento di Fisica “G.Galilei”, Via Marzolo 8, 35131 Padova, Italy

E-mail: dorigo@pd.infn.it

Abstract. The CDF and DØ collaborations at the Tevatron have been producing exquisite precision measurements on high-P_T physics with their large datasets of $p\bar{p}$ collisions. During the few years that divide us from the start of operation of the Large Hadron Collider experiments at CERN, a lot can be done besides improving the measurement of accessible observable quantities, to prepare the ground for an easier and more successful exploitation of the forthcoming LHC collisions.

Foreword

Allow me to start these proceedings by thanking the organizers of the Corfu 2005 conference for their effort, and for putting together a successful mix of topical conferences and schools in a lovely venue. The relaxed atmosphere, the careful organization, and the beautiful setting conspired to make the meeting a productive and very pleasant one.

The present document summarizes the review I gave in Corfu last September on the status of high transverse momentum physics at the Tevatron. The review focused primarily on measurements which are both of current interest at the Tevatron, and of future relevance in the forthcoming years, when a migration of experience, analytical effort, and eventually results will occur towards CERN, where the Large Hadron Collider (LHC) is being built.

In my talk I did not make any attempt at being exhaustive in the choice of discussed topics –I did not deal with QCD measurements or exotic searches– nor in the coverage of those I did discuss. I also felt free to upset the usual balance of an equal share of advertisement of the results of the two Tevatron collider experiments: I cited mostly analyses performed by CDF, which I of course know more in detail, being a member of that collaboration.

The same approach will be offered here. I however made my best to provide updated results, where CDF or DØ produced anything new since September 2005. My excuses are herewith offered in advance to anybody who feels their favourite analysis has been neglected: this is by no means a complete review of current results, nor a showroom of the best ones, but rather a discussion of general topics that appear of relevance in the few years that will bridge us from the Tevatron to the LHC era.

It is indeed of paramount importance for the future of high-energy physics in the 21^{st} century to not only treasure the experience gathered by analysing 2 TeV proton-antiproton collisions during the last 20 years at the Tevatron, but also to identify well in advance those aspects that make a difference when going from 2 to 14 TeV, and specifically the ones which will be most critical for a successful exploitation of the LHC data.

Of course, several studies have been carried out in the past with the above goal in mind. The present, however, provides us with Tevatron data in large amounts, and the statistical precision with which CDF and DØ are measuring physical quantities is now forcing the two experiments into putting a major effort in investigating new ways to reduce the by now dominant systematic uncertainties.

Now is therefore as good a time as any to summarize the status of our learning curve in the preparations for the LHC era.

1. Introduction

1.1. The present

The Tevatron accelerator has been subjected at the turn of the millennium to a massive upgrade, with the construction of an entirely new ring, the Main Injector, and several improvements in the facility producing and storing antiprotons – the most challenging part of the whole project.

A sketch of the Run II setup of the Tevatron accelerating complex is shown in Fig. 1.

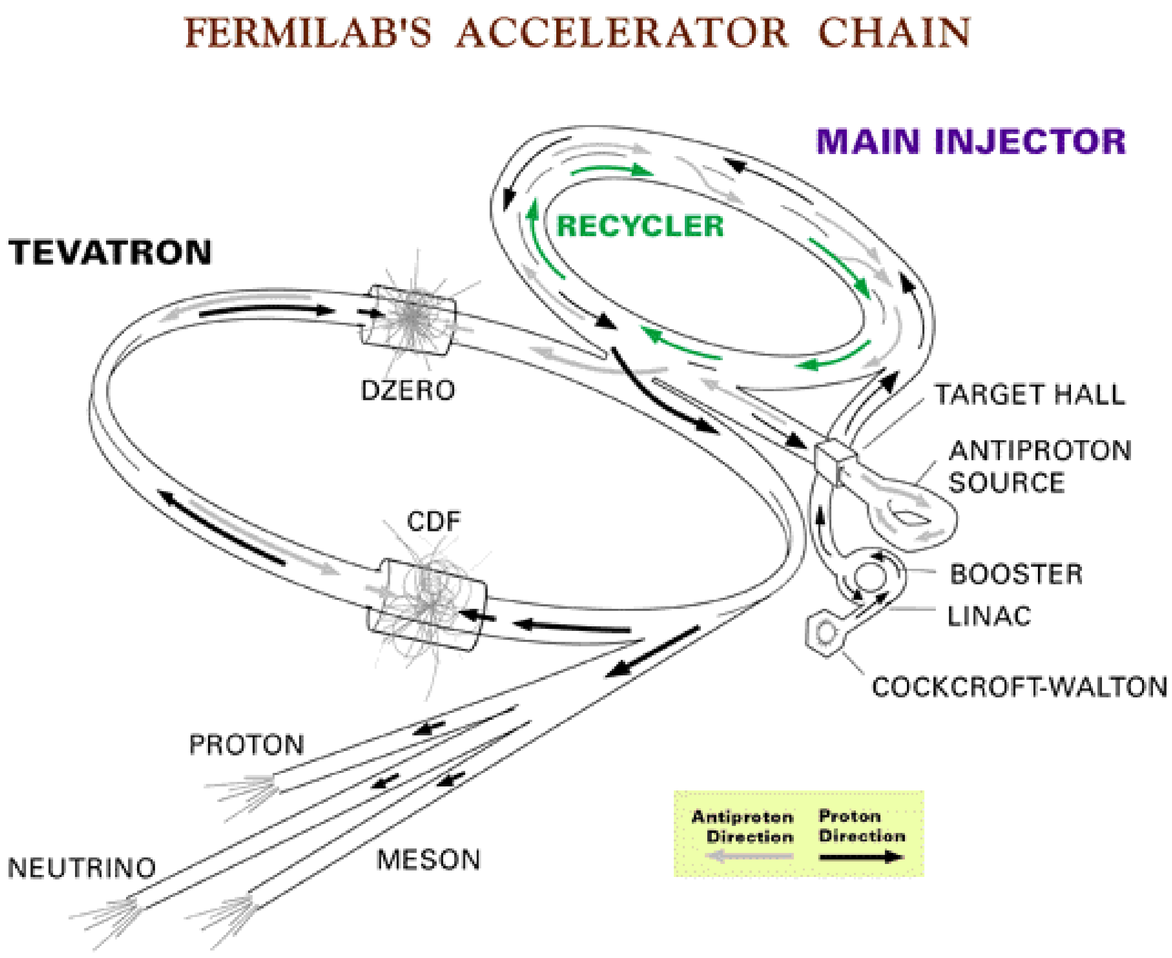

Figure 1. *Sketch of the Tevatron accelerator facility.*

A modest increase in beam energy –from 900 to 980 GeV– was the by-product of an upgrade of the accelerating cavities. The Tevatron upgrade did not aim at achieving the maximum possible center-of-mass energy so much as at securing the best operating conditions which would guarantee the machine to consistently deliver the highest possible instantaneous luminosity, a crucial ingredient to keep hopes alive for a Higgs boson discovery, and for the measurement of mixing parameters of B_s mesons, the other main goal for Run II of the CDF and DØ experiments –now successfully achieved. The 9% increase in center-of-mass energy does grant a $\sim$ 25% increase in production rate of heavy particles such as the top quark or the Higgs boson, but the impact that a larger number of protons and antiprotons and a faster rate of data collection have on the discovery reach of the Tevatron experiments in Run II is more dramatic. The Tevatron has recently surpassed the peak luminosity of $1.8 \times 10^{32} cm^{-2} s^{-1}$ (see Fig. 2), and has been consistently delivering steady beam to the experiments. An integrated luminosity of about $1.5 fb^{-1}$ per experiment has been collected at the time of writing.

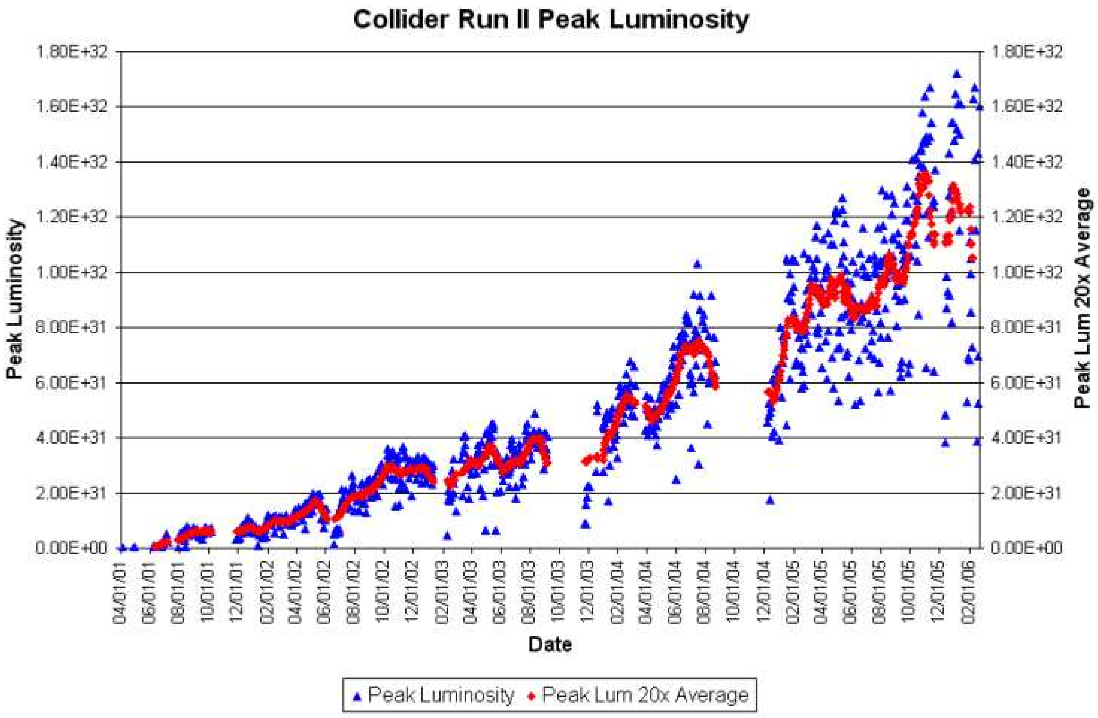

Figure 2. *Peak luminosity of Tevatron runs from 2001 to 2006.*

During 2006 a few crucial upgrades are being completed following the plan of increase of machine luminosity, whose critical ingredients are the efficient production, storage, and transfer of antiprotons. The two principal improvements are electron cooling of the antiproton beam and an increase of the stacktail bandwidth.

Electron cooling [1] has been recently demonstrated in the recycler ring by merging a 4.8 MeV beam of electrons with the 8.9 GeV beam of antiprotons. Because of the different masses, particles in the two beams move at the same speed; the electron current stabilizes the antiproton beam, reducing the longitudinal spread in antiproton velocities. An increase in the capability of antiproton stacking, through an upgrade of the accumulator stacktail cooling system, is expected to significantly improve the speed of antiproton collection and the resulting amount of available particles for Tevatron collisions.

If the described upgrades should not work as planned, the Tevatron will still be able to deliver a total of $4 fb^{-1}$ to each collider experiment by 2009 –what has been called *base plan.* But if the upgrades will produce the desired effect, the design luminosity of $8 fb^{-1}$ is likely to be collected by that date (see Fig. 3). This latter *design plan* might change the perspective of Tevatron physics in Run II, giving CDF and DØ significant chances of a light Higgs boson discovery before or in coincidence with a LHC observation.

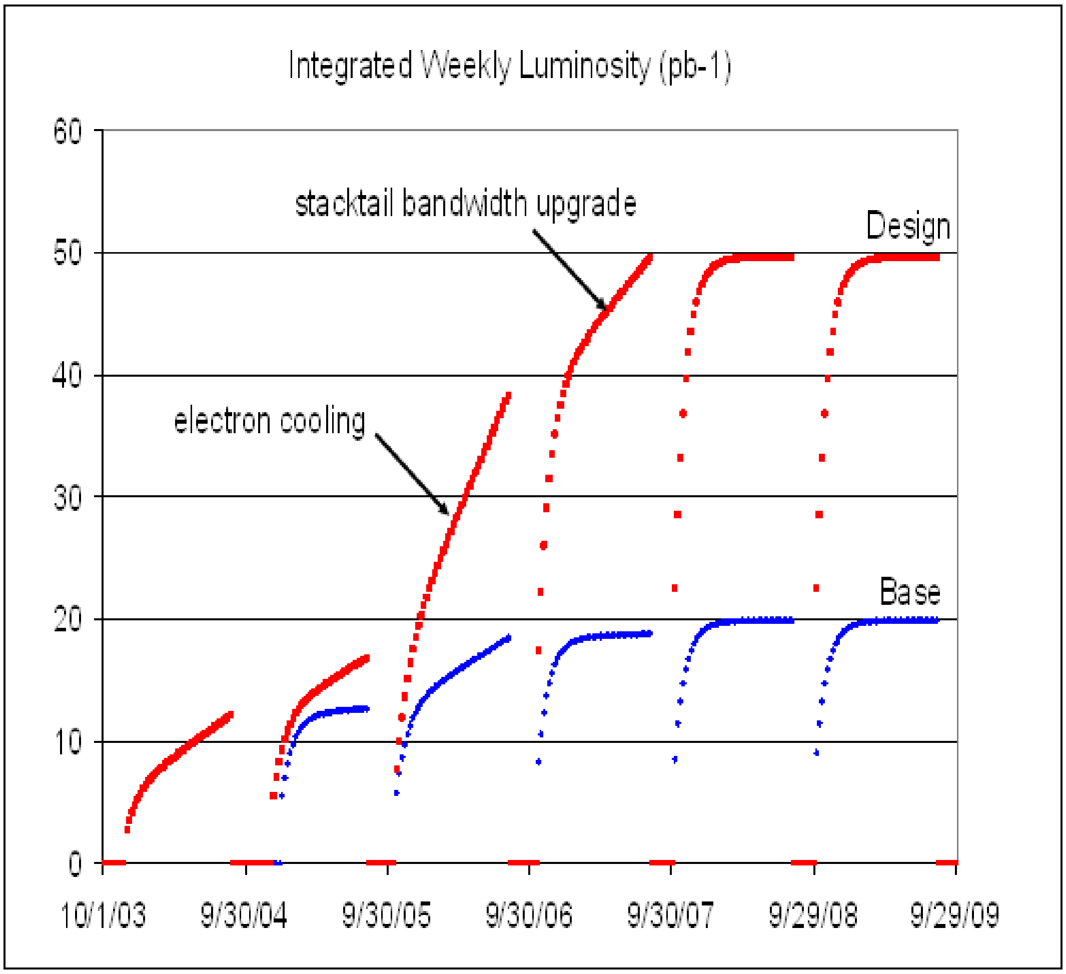

Figure 3. *Predictions for weekly integrated luminosity delivered by the Tevatron accelerator. The design plan corresponds to a total integrated luminosity of* $8fb^{-1}$ *by the end of 2009, while the base plan corresponds to* $4fb^{-1}$.

1.2. The future

The Large Hadron Collider (LHC), the accelerating complex in construction at the CERN laboratory in Geneva, is a truly daring enterprise, attempting to scale the two significant machine design parameters –beam energy and luminosity– up by an order of magnitude from the previous records reached by its predecessor, the Tevatron collider of Fermilab.

From the 980 GeV beams of protons and antiprotons of the Tevatron to the 7000 GeV beams of protons of the LHC, the leap forwards is giant. It entails the construction of 1232 superconducting magnets to provide the necessary bending force in the CERN 26.7 km tunnel, which until 2002 hosted the LEP II accelerator. The total stored beam energy at the design luminosity of $10^{34}cm^{-2}s^{-1}$ equals the kinetic energy of a loaded Airbus A340-200 at landing speed.

Challenging is also the design and construction of a system capable of running with 2808 $25ns$-spaced bunches of protons, achieving beam stability throughout the LHC tunnel, and squeezing the bunches transversely to a diameter of $\sim 34\mu m$ in the center of the experimental facilities.

Together with the technical challenges involved in the construction of the accelerating complex, the construction of the CMS and ATLAS experimental apparata are also quite demanding.

CMS and ATLAS were born originally different in a few key design features, but gradually became more similar as the first blueprints evolved into the commissioning phase, in a process of dynamical likening that was already observed between DØ and CDF a decade ago.

The focus of the experiments, it appears, has gradually shifted from a marked accent to muon detection –with the aim of observing the ultra-clean signature of Higgs boson decay to a pair of Z bosons, $p\bar{p} \to H \to ZZ \to \mu\mu\mu\mu$– to a greater versatility. The motivation of that shift was the need to not only ensure detection of a Higgs boson whatever its mass, but also to do it with the smallest possible amount of data –*id est*, in the shortest possible time. Moreover, if the original motivation for building the experiments was principally the detection of the Higgs boson, maintaining a rich physics program and constant financing for many years is a more important item in the agenda once construction funds are secured: the Higgs discovery is by now practically given for granted, and the discovery of supersymmetry is the real goal for LHC.

As we approach the starting date of the first collisions, most of the construction problems are on the way of being successfully solved. The LHC must not fail: the high energy frontier will rely on that machine for the next ten years. Interestingly, a strong commitment to make the CMS and ATLAS experiments successful enterprises has been demonstrated recently also by the United States, where the active participation in the experiments has been dubbed "strategic" for the plan of bringing back the leadership in frontier particle physics to the american soil [2].

1.3. From the present to the future

For an experimentalist, the best way to exploit these few years that divide us from the time when the first data will be collected by the LHC is to prepare the ground for their successful exploitation, thinking in advance at what will be the dominant sources of uncertainty to the most intriguing measurements, and what solutions can be cooked up to reduce them.
A specific example of this preparatory action is the study of the effect of trigger selections to the calibration datasets which will be needed by many precision measurements. Take the top quark mass as a benchmark: in 2008 the relative uncertainty on this fundamental parameter of the Standard Model –after the combination of CDF and DØ results– will be likely smaller than 1.5 GeV, and quite possibly smaller than 1 GeV (see Fig. 4). If LHC experiments mean to improve still further the knowledge of that number, they will need a very careful planning of the reduction of systematic uncertainties from the jet energy scale and from all other sources. As far as the jet energy scale is concerned, the Tevatron experience shows that large samples of dijet production events are needed for an accurate modeling of detector effects, and as many photon-jet events as possible for checks of the systematic uncertainty. These "calibration samples" are taxing for the total data acquisition bandwidth, but they are really necessary. Jet energy scale systematics are discussed with some detail in Sec. 3.1.

1.4. Plan of the writeup

The present writeup will attempt at offering some insight on several important challenges in the use of Tevatron results, data, and experience to prepare the ground for the LHC.

Section 2 will provide a short overview of the CDF and DØ detectors. In Section 3 I will discuss some of the most important methods currently used to perform precise measurements of

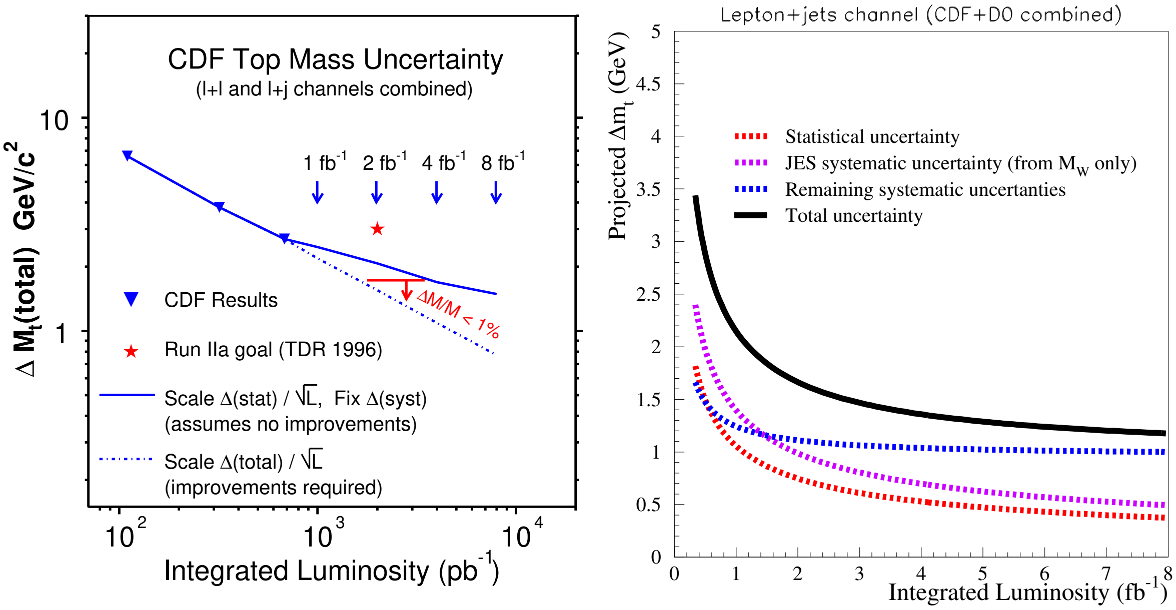

Figure 4. *Left: expected top mass uncertainty from combined dilepton and single lepton CDF measurements, as a function of integrated luminosity in Run II. Right: expected top mass uncertainty from lepton plus jets events, CDF and DØ experimental results combined, as a function of integrated luminosity per experiment.*

hadronic jets and efficient b-tagging, which are two critical ingredients to most of the high-P_T physics program of the Tevatron experiments.

In Section 4 the status of Higgs boson searches ongoing in CDF and DØ data will be discussed, along with some speculation on the possible scenarios that the LHC experiments will be dealing with. Section 5 will discuss a few selected issues in top quark physics, and the challenges posed by precision measurements of important quantities in the top sector.

Section 6 will deal with electroweak physics measurements that may not only help improve the picture of Standard Model physics before the LHC, but also provide some opportunities to reduce key systematic uncertainties on precision measurements by CMS and ATLAS.

A few concluding remarks are provided in Section 7.

2. Selected information on the Tevatron detectors

An overview of the CDF and DØ detectors for Run II at the Tevatron can be found in [3]. In what follows I will briefly mention some significant upgrades of benefit for the high-P_T physics program of the two experiments.

2.1. CDF

CDF (see Fig. 5) has been massively upgraded from Run I, to meet the more stringent requirements of Run II conditions, and to increase the discovery potential both in high-P_T and B-physics.

The smaller time interval between bunch crossings (which went from $3.5\mu s$ to $396ns$, but was originally intended to reach $132ns$) mandated the construction of a much faster drift chamber, the Central Outer Tracker (COT). The larger backgrounds and higher rates also dictated a

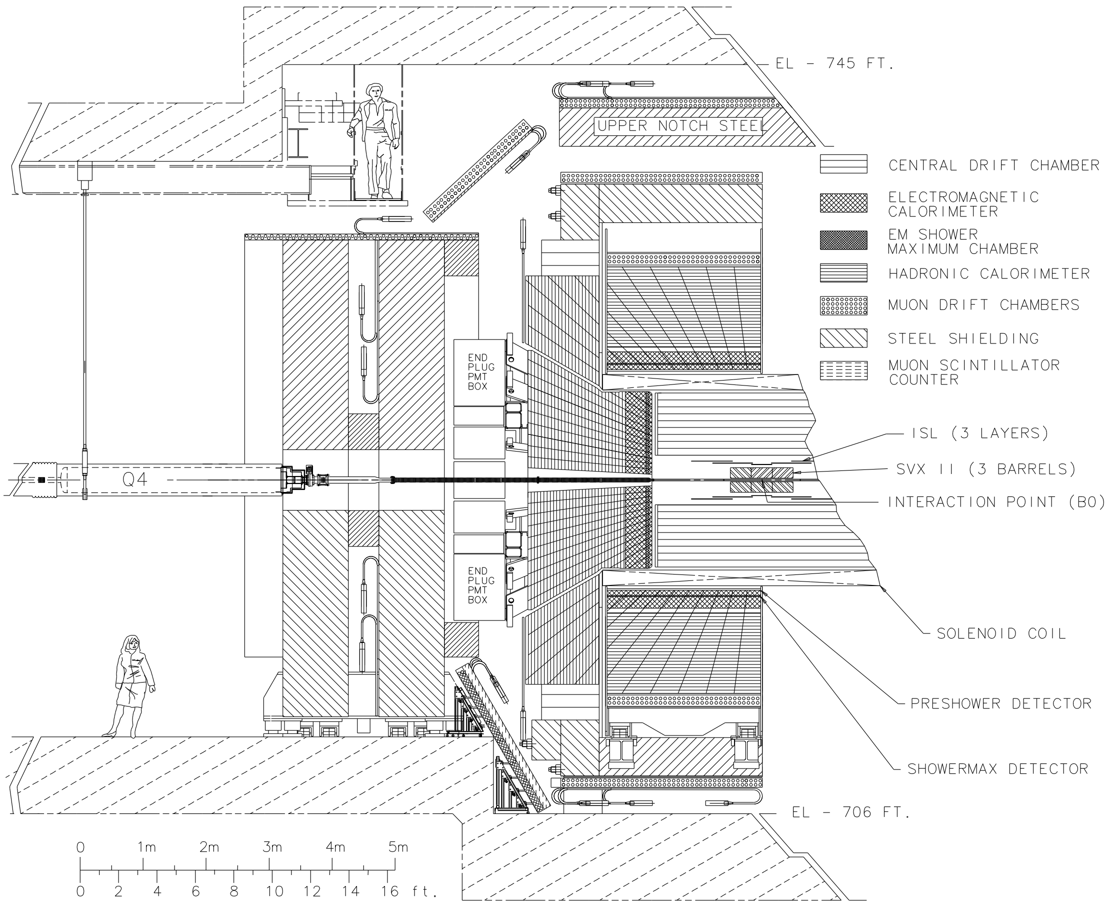

Figure 5. Cut-away view of the CDF detector.

replacement of forward calorimeters (which had gas as active medium in Run I) and a complete overhaul of data acquisition electronics.

A wider acceptance to electrons and muons, which is beneficial for the collection of top and Higgs decays, was achieved by the installation of new forward muon detectors and a more redundant and extended inner silicon tracking, now based on seven layers of strip sensors. CDF now measures W decays to rapidities in excess of $\eta = 2$ (see Sec. 6.1), with a significant acceptance increase for top quark decays and more power to constrain quark parton distribution functions from boson production asymmetries.

Of particular relevance for the present review is also the completely new device that was designed and built to achieve online silicon tracking at trigger level 2: the Silicon Vertex Tracker (SVT), capable of measuring track momentum, azimuth, and impact parameter with precision close to that attainable offline.

The SVT works by performing a linearized $R-\phi$ fit of track hits in four silicon layers together with a further "hit" at larger radius obtained from fast track reconstruction by the COT. Track candidates are identified by comparing hit patterns to a predetermined array of possible roads stored in associative memory banks. The 12-fold ϕ symmetry and six-fold z modularity allow for a natural parallelization of the task, and the parameters of central tracks are precisely obtained with 90% efficiency in about 10 microseconds. In particular, the impact parameter is determined with a $45\mu m$ resolution. The triggering capabilities of the SVT have enabled CDF to collect huge samples of fully hadronic B hadron decays: the recent precise measurement of B_s mixing frequency achieved by CDF is almost entirely due to the SVT.

2.2. DØ

The most substantial improvement of the DØ detector for Run II was the insertion of a two Tesla superconducting solenoidal magnet, which now provides it with charge and momentum measurement capabilities. Inside the magnet, DØ installed a scintillating fiber tracker (see Fig. 6), organized in eight concentric cylinders. Light from the fibers is transported to solid-state light detectors of very high gain.

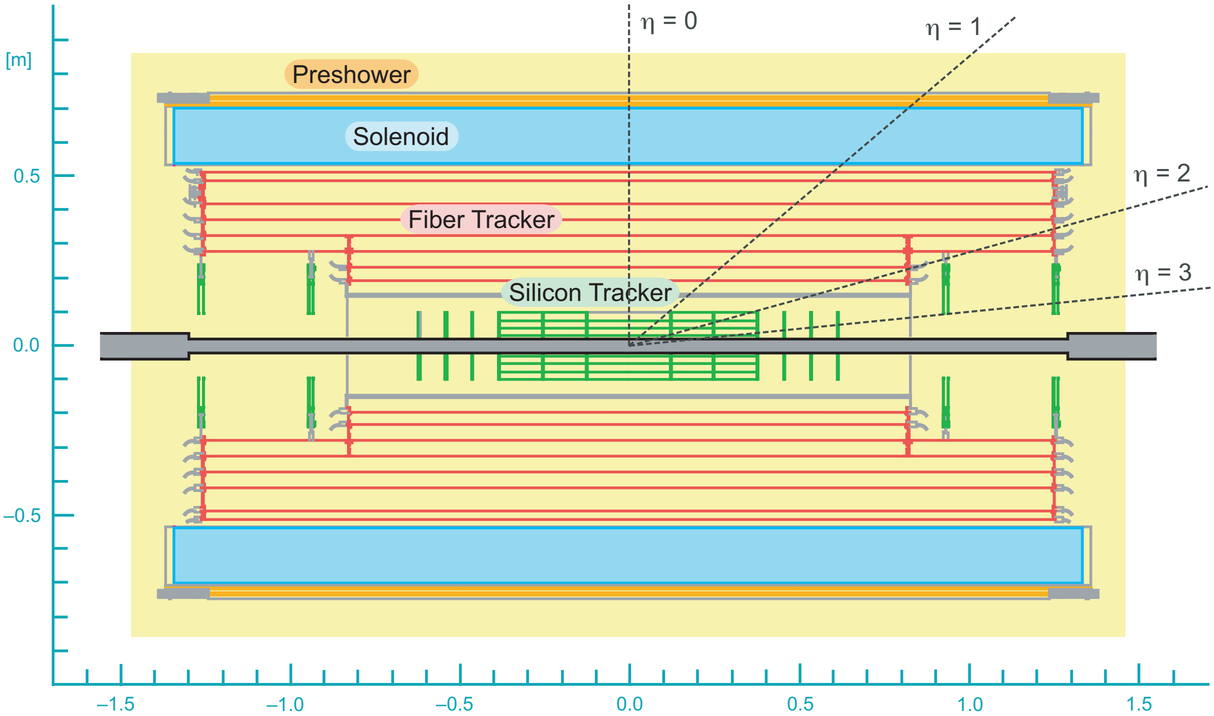

Figure 6. A view of the new tracking system of the DØ detector.

A redundant system of silicon microstrip detectors provides precise position measurement to enable a high-efficiency b-tagging of hadronic jets through the measurement of track impact parameter. Six barrels of silicon sensors organized in four concentrical layers provide coverage for central tracks, while a total of sixteen silicon disks allow reconstruction of large rapidity tracks.

The main addition to the calorimeter system of DØ was the installation of central and forward preshower detectors, whose purpose is to improve the trigger and offline purity of electrons and photons. The muon system was also upgraded to maintain an efficient operation in the higher fluxes of Run II. Mini-drift tubes composed of three planes, one in front and two in the back of the toroid magnets, were installed in the forward region.

3. Tools for precision high-P_T physics

3.1. Measuring hadronic jets

Hadronic jets are the most common and obvious phenomenon one can observe in high energy hadronic interactions; however, a precise definition of a jet that allows a unambiguous measurement of its properties is by no means trivial, and to some extent depends from the use one needs to make of the extracted measured quantities. If, for instance, one wishes to reconstruct the decay of a heavy object, one needs a jet identification algorithm which allows the best possible one-to-one matching with the quarks originated from the hard subprocess; other requirements in that case range from an optimization of the resulting signal to noise ratio, to an easy computation of systematic uncertainties affecting the energy measurement.

The choice resulting from the criteria mentioned above may be quite different from the ones which are most convenient for a differential cross section measurement of quantum chromodynamics, where the focus is primarily on the easiest, most accurate comparison to theory. Furthermore, a general requirement of jet identification algorithms is portability: the reproducible behavior of a procedure applied to data coming from different experiments is welcome when one wishes to combine results.

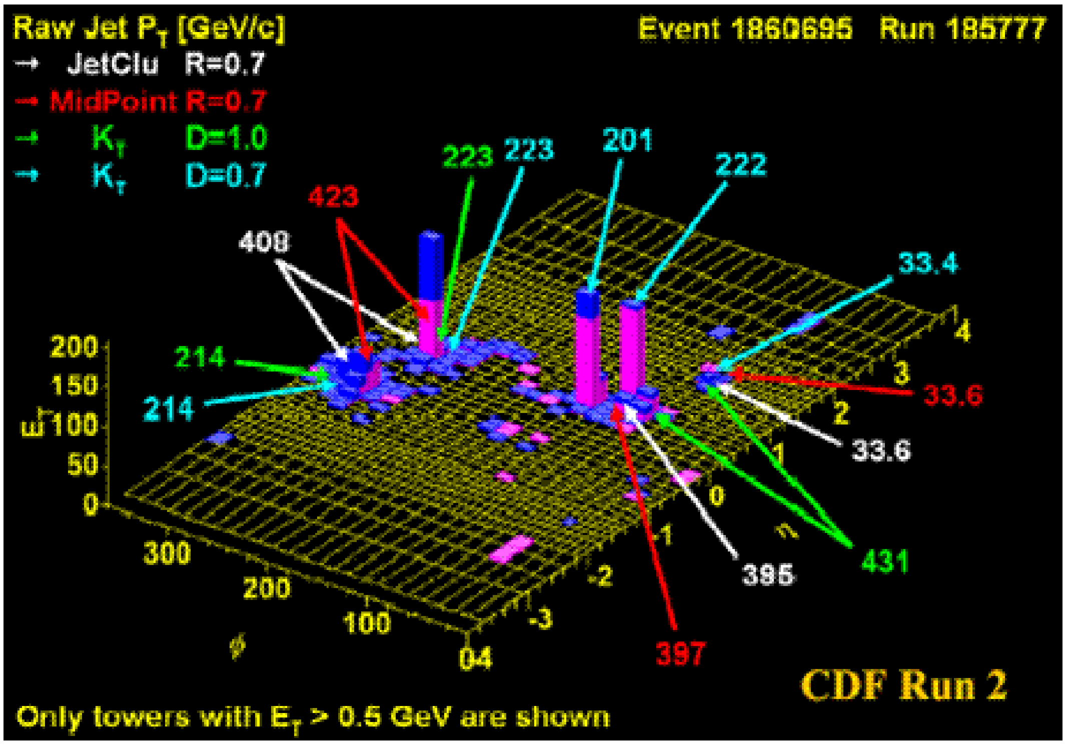

Figure 7. One event, three algorithms: the standard cone algorithm identifies four jets (white arrows) in this energetic multijet event collected by CDF. The same objects are reconstructed by the Midpoint algorithm, although measured energies differ. The K_T algorithm can correctly "split" the two narrow jets on the right, if ran with a suitable "cone" parameter.

The CDF and DØ experiments have implemented three different software algorithms for jet reconstruction: a standard iterative cone algorithm, a variant called *midpoint*, and a version of the K_T algorithm usable in hadronic environments. Fig. 7 shows the lego plot of calorimeter energy measured by CDF in a high-P_T multijet event, and the interpretation of energy deposits as hadronic jets obtained by the use of these three different algorithms.

The cone algorithm is based on what is conventionally called the "Snowmass Accord" [4]. In CDF the list of all calorimeter cells above a fixed threshold in transverse energy, $E_T > 0.1$ GeV, is ordered by E_T, and a circle of predetermined radius is drawn in the $\eta - \phi$ space around the most energetic cell. The radius $R = 0.4$ is used for the reconstruction of the decay of heavy objects such as the top quark, $R = 0.7$ is a good compromise between a correct identification of the event topology and the measurement of soft gluon radiation off the final state partons, and $R = 1.0$ is only useful for dijet or photon-jet final states.

All cells within the circle are removed from the list, and a E_T baricenter is computed for the circle from the included cells. The highest-E_T cell remaining in the list constitutes the center of the next circle, and the clustering is repeated until no cells are left which have E_T above a "seed" threshold (typically equal to 1 GeV). The resulting circles are then redrawn around their own baricenter, sometimes including new cells or losing some; the procedure is repeated until the configuration is stable. A prescription for splitting or merging clusters takes care of cases when two circles partially overlap, and is based on the fraction of energy shared. From the final list of clusters the energy and direction of each jet is obtained.

A specialization of the cone algorithm described above is called *Midpoint*, and is the default choice in DØ . The midpoint algorithm adds seeds for the clustering at the middle point between the original clusters, thus avoiding the shortcomings of the splitting and merging prescription of the iterative cone procedure which make comparisons to theory difficult.

A different concept is the basis of the K_T algorithm, which uses energy along with spatial separation to define the distance between energy depositions, and allows more precise comparisons with analytical calculations, being unaffected by infrared and collinear singularities of soft parton emission. For that reason, the K_T algorithm is mainly of benefit to QCD cross section measurements.

When faced with the measurement of the kinematics of hard parton emissions based on a reconstruction algorithm such as the ones described above, one has to deal with two distinct issues: the precise determination of a energy scale, and the achievement of the best possible energy resolution.

Knowledge of the jet energy scale k of hadronic jets allows to calibrate the detector response such that a sample of partons of a given energy E_{true} will be reconstructed with that same energy, *on average*. A shift of the average $\bar{E}$ from E_{true} signals a deviation of the scale from unity – and the need for a general correction $E' = kE$, with $k = E_{true}/\bar{E}$. It follows that the smaller the error on the value of k, the more precise will be any measurement of physical quantities derived from jet energies. In Sec. 5.3 a quantitative example of this correspondence will be given for the case of the top quark mass measurement by CDF.

A precise knowledge of k is not enough, however. While k determines the *collective* behavior of the energy measurement of jets we perform in our detector, the resolution σ – which can be defined as the width of a gaussian distribution of measured energy E from jets of the same true energy E_{true} – determines the typical deviation of the measured energy of *any given jet* from its expected value $\bar{E}$. A small value of jet resolution is a big asset for a high-energy experiment, since it improves any measurement affected by backgrounds, which become easier to handle. Typically, the signal of a jet-decaying resonance will increase its significance linearly with a decrease of σ: for Higgs boson searches at low mass, when the decay $H \to b\bar{b}$ is sought, the dijet mass resolution is one of the critical parameters. In Sec. 3.3 the matter is discussed in detail.

3.2. Jet calibration and determination of the energy scale

From an experimental standpoint, it is important to realize that the result of a jet measurement is affected by a multitude of effects of different origin. These effects need to be addressed separately, to allow uniform definitions across different experiments and comparisons with theory.

The prime example of a detector-specific effect needing compensation is the non-uniformity of the detector response. Real detectors are always non-uniform in their mechanical construction, in the amount and location of dead channels, in the material budget as seen from the interaction region. Although a simulation of the apparatus may help us to understand the dominant non-uniformities, a detailed accounting of all effects requires the study of real data. With dijet events it is possible to use one jet to probe the detector response as a function of its relevant variables (such as rapidity and P_T), when the other jet (the one responsible for triggering the event) is constrained to be measured in a well-controlled region.

By computing the response function f, defined as

$$< f(\eta, P_T) >= \frac{2}{N}\Sigma \frac{P_T^{trigger}-P_T^{probe}}{P_T^{trigger}+P_T^{probe}}$$

for a large set of jet pairs and with the probe jet spanning several bins in P_T and rapidity, one obtains a map of the detector output, which can be subsequently used to equalize the response. The P_T binning is necessary, since as their P_T grows jets become narrower, and they probe smaller scales of non-uniformity of the detector. A method roughly equivalent to the one discussed above involves the use of the fraction of missing transverse energy projected along a jet direction. Again, what one measures is a systematical bias of the response of different parts of the detector as a function of jet P_T and rapidity.

The CDF collaboration extracts their relative correction function using the dijet balancing technique, while DØ uses the missing E_T projection method. The relative response is shown for both detectors in Fig. 8.

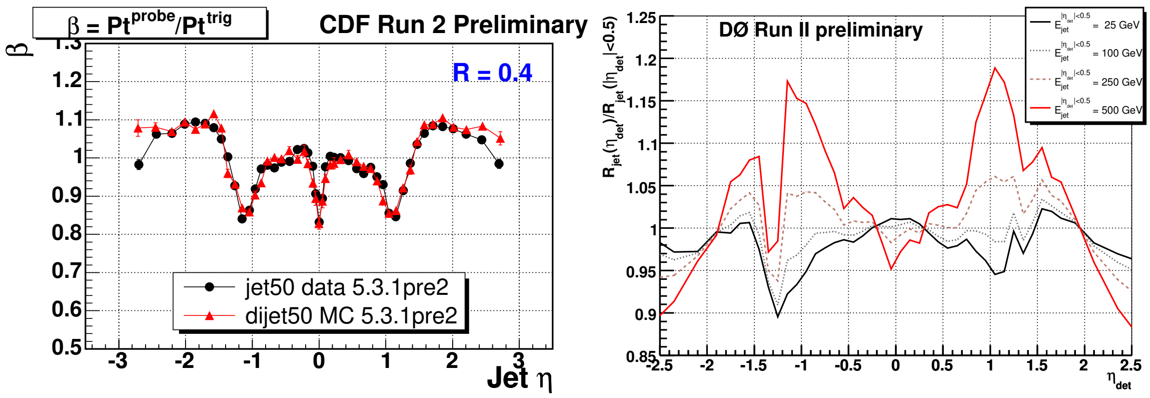

Figure 8. Left: a rapidity-dependent jet P_T correction factor extracted by CDF from dijet balancing studies. Right: a similar function obtained by DØ with the missing E_T projection method.

Another method must be devised to account for energy collected in the clustering cone from pile-up interactions occurring during the same bunch crossing. Pile-up energy is on average a linear function of instantaneous luminosity, but only through the number of pile-up interactions. It is therefore much better to correct jets on an event-by-event basis, by determining the average energy deposited in a random cone in the calorimeter (away from real jets) as a function of the number of primary interactions reconstructed through vertexed charged tracks.

A similar kind of random contribution to jet energy comes from a different origin: the same hard interaction that produces the jet activity may radiate additional energy through the so-called *underlying event*, which has to be understood as the combinative effect of proton remnants recombination and additional hard or semi-hard interactions by the spectator partons. An average correction for this effect can be obtained by computing the energy deposit in cones in a region azimuthally orthogonal from the leading jets in generic QCD events.

Another small correction may be applied to account for energy flowing out of the clustering circle: this is called *out-of-cone correction* and is of course dependent on the choice made for the clustering radius R.

The most important effect for a calorimeter energy measurement is however the difference in response to particles creating electromagnetic showers in the first few radiation length of calorimeter material – essentially photons from π° decay, and electrons if there are any – and charged hadrons (mostly protons and light charged hadrons), which are measured predominantly in the hadron calorimeter. The energy of electron-like showers is determined with high precision in the electromagnetic section of the calorimeter, while hadronic showers generate nuclear interactions that cause substantial energy loss through a multitude of effects.

To determine the correction factor to apply to the measured energy and obtain the most probable value of the originating stream of *stable* particles (stable in the sense that their lifetime is long enough to allow detection before decay), a Monte Carlo simulation is used in CDF. The simulation is tuned with the known single-particle response functions determined from dedicated runs and test beam studies. With large samples of simulated jets a mapping function that relates the observed energy to the energy of the particle jet is extracted.

Once all correction factors and offsets are applied, the jet energy scale can be checked with events in experimental data where one jet recoils against an energetic photon (or leading neutral particle). The electromagnetic shower is well measured in the inner sections of the calorimeter, and the recoiling jet energy scale can be tested with good accuracy.

An uncertainty in the jet energy scale can then be determined by comparing the offset between data and Monte Carlo, if the Monte Carlo jets have been subjected to the same treatment as jets in experimental data.

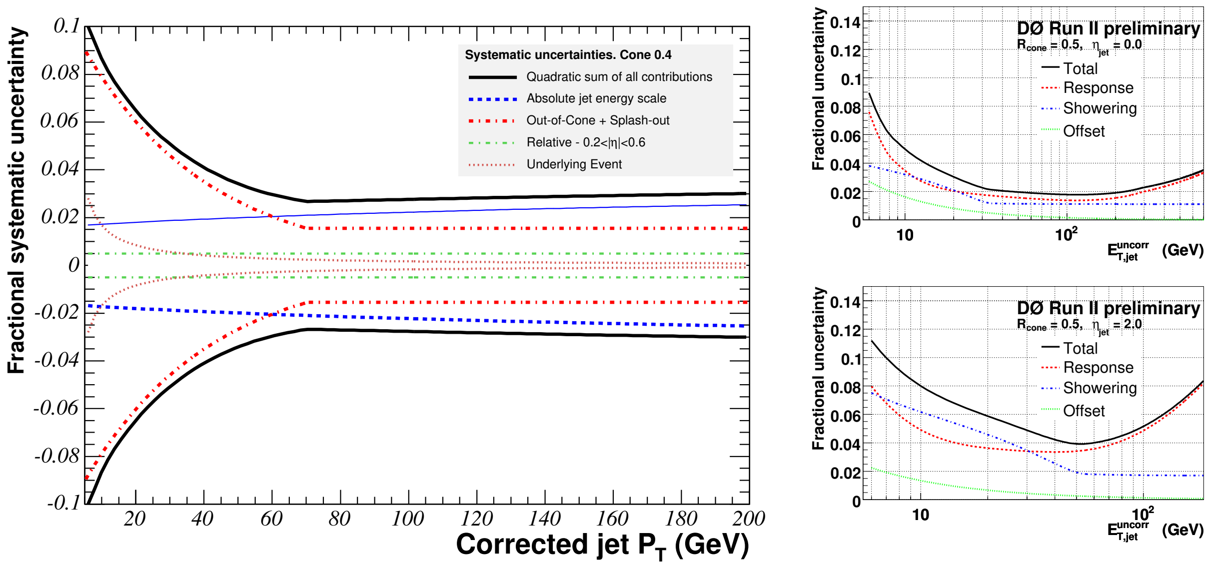

Figure 9. Left: total systematics on jet energy measurement as a function on jet P_T at CDF ($R = 0.4$, all jet rapidities). Right: total systematic uncertainty in DØ ($R = 0.5$, two different bins of jet rapidity).

The level of uncertainty in the determination of the jet energy scale at the Tevatron experiments is below 3% for jet $P_T > 50$ GeV (Fig. 9), and is expected to decrease further as more data –particularly photon-jet events– are collected. The large samples of single lepton decay of $t\bar{t}$ pairs collected by the experiments have also allowed to cross-check the energy scale by using the $W \to jj$ resonance in top decay.

For a complete review of the determination of jet energy scale in CDF see [5]. The jet energy scale correction in DØ is described in [6].

3.3. Improvement of jet energy resolution

The resolution of jet energy measurement plays an increasingly important role as larger datasets of high P_T processes are collected at the Tevatron. It is of course a critical parameter in those searches for small cross section signals of hadronic resonances, such as a light Higgs boson; but it also affects significantly the accuracy of several precision measurements, and specifically wherever the kinematics of final state quarks requires to be pictured with accuracy. In particular, the precision of all jet-based top quark mass measurements also depends significantly on the accuracy with which final state partons are measured.

CDF and DØ have taken seriously the challenge to improve the jet energy resolution. The Higgs Sensitivity Working Group (HSWG), a joint CDF-DØ venture, spurred studies aimed at demonstrating that a 10% relative resolution on the dijet invariant mass for pairs of b-jets was achievable in both detectors [7]. The issue, however, does not involve only b-jets, which are less well measured but quite special in their characteristics –and therefore easier to improve.

A working group in CDF identified three main candidates for the improvement of the resolution on generic jets: the **H1 algorithm**, which uses the momentum of charged tracks instead of hadronic energy depositions in the calorimeter when possible; **JetCor2k**, an algorithm which attempts to perform a complete classification of energy deposits in calorimeter towers into photon-like, track-like, mixed, and unassigned, thereby correcting differently each of them; and the **Hyperball algorithm**, which attempts to use all jet observables –even ones which should have little information on the jet energy measurement error– to exploit the intercorrelation among these variables to determine the average P_T error of jets. A fourth candidate –and maybe the most obvious– has been under development by both DØ (for the HSWG) and later by CDF: a **Neural Network** classifier. Neural Networks are usually thought of as signal discrimination tools, but they are very flexible. In the case of jet energy correction, the network is trained to recognize jet energy given the input variables: it thus acts as a multi-dimensional non-parametric fit.

Here I will just describe with some detail the Hyperball algorithm, which I developed for the improvement of the Higgs mass resolution.

The Hyperball algorithm is nothing more than a fancy prescription for computing averages. Let us define a scalar function Δ as the average difference between the transverse momentum P_T^q of a final state quark and the measured P_T^{jet} of the resulting calorimeter cluster. $\Delta(\vec{x}) = P_t^q - P_T^{jet}(\vec{x})$ can be thought to be a continuous function of all measurable jet quantities $\vec{x}$ our detector is capable of providing: for instance, $\Delta(\vec{x})$ is usually positive for jets showing a ratio between total track momentum and P_T^{jet} larger than unity, for in that case the calorimeter measurement is likely to be underestimated. Another example is the predictive power of a larger-than-average ratio between jet mass M^{jet} and P_T^{jet}, which can indicate either that the core of the jet has been undermeasured –for instance, due to the jet falling into a crack of the calorimeter– or that the energy far from the jet core has received extra energy, maybe from other jets or pile-up. Normally, one would be unable to decide which of the two causes is yielding a large M^{jet}/P_T^{jet} ratio, and a correction would be impossible; but in a multi-dimensional space, where the charged fraction is also considered, the two cases get easily separated.

It is obvious that a unlimited amount of simulated jets would allow $\Delta(\vec{x})$ to be known with arbitrary accuracy: averaging $\Delta(\vec{x})$ for all jets with identical measured characteristics to the one under scrutiny enables one to compute an optimal corrected value $P_T' = P_T^{jet} + \Delta$. The Hyperball algorithm takes care of using to the fullest the limited statistics available of simulated jets. A generalized distance $R(\vec{x})$ in the multi-dimensional space spanned by all jet observables $(\vec{x})$ is defined such that those coordinates along which $\Delta(\vec{x})$ has the largest gradient weigh the most: for jets 1 and 2,

$$R(\vec{x}(1) - \vec{x}(2)) = \sqrt{\Sigma_i (\frac{\partial \Delta}{\partial x_i})^2 \times (x_i(1) - x_i(2))^2}.$$

With the above definition, one can then inflate a *hyperball* –a region of constant R– around the coordinates $\vec{x}(0)$ of the jet to be corrected, enclosing within it a suitable number N of simulated jets whose characteristics will be most similar to it, from the point of view of the value of Δ. Δ can then be computed as the average of the jet measurement error inside the hyperball, weighted with the inverse of R^2.

Improvements of as much as 30% have been predicted on the resolution of b-quark jets in the range of interest for the search of top quarks and light Higgs bosons. The algorithm is currently under testing with the recently observed signal of $Z \to b\bar{b}$ decays in CDF data (see Sec. 4.1).

3.4. b-jet issues

Jets originated from b-quark fragmentation possess unique characteristics that constitute both a challenge and an opportunity for high-P_T physics at hadron colliders, regardless of the center-of-mass energy. Weak couplings make b-jet production rate in electroweak production processes larger, for any given Q^2, than in QCD processes, so that their identification usually eases signal extraction.

An effective identification of b-jets from generic jets is actually made possible by the small value of the Cabibbo-Kobajashi-Maskawa (CKM) mixing matrix element V_{cb} and consequent long lifetime of B hadrons, which allows a reconstruction of the secondary decay vertex; and also by the large b-quark mass, which yields a significant fraction of semileptonic decays.

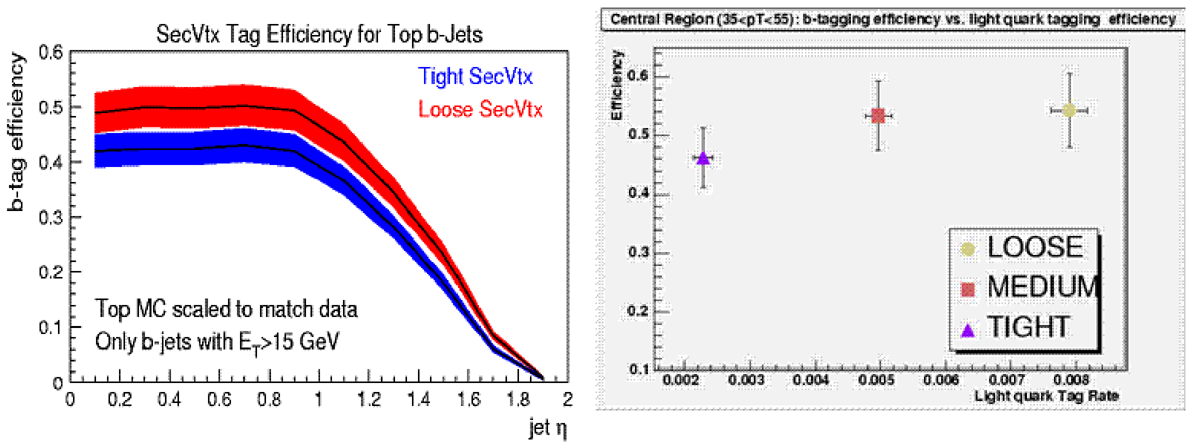

Figure 10. Left: efficiency of the loose and tight secondary vertex tagging algorithm by CDF as a function of jet rapidity. Right: the b-tagging efficiency of three versions of the vertex tagging algorithm developed by DØ are shown as a function of fake rate.

CDF and DØ have put a lot of effort into maximizing their b-tagging capabilities, developing several tagging strategies based on the main characteristics of b-quark decay. Performance of the secondary vertex tagging algorithms are similar in the two experiments, which developed both a *tight* and a *loose* version of the identification procedure; the *loose* version is typically used to retain high efficiency for double b-tag when reconstructing signals nominally yielding two b-jets, such as decay of $t\bar{t}$ pairs or light Higgs bosons. The efficiency to correctly identify a b-quark ranges from 40 to 50% for central jets, with fake rates of less than a percent (see Fig. 10); as jet rapidity increases, a deterioration of the efficiency is observed in both detectors, although the silicon disks of the DØ detector appear effective in keeping a reasonable efficiency out to $|\eta| < 2.0$.

As an alternative to fitting the tracks to a common secondary vertex, one can determine the global probability that those tracks all originate from the primary interaction vertex, by comparing track impact parameter d_0 with expected resolution functions; if properly computed, the probability P is flat for a sample of tracks originated from non-heavy flavor jets. P is a continuous variable which allows a dialing of the desired b-quark efficiency, by setting $P < P_{max}$ (typically $P_{max} = 0.01$), and the resulting fake rate (the fraction of tagged light flavor jets) which, to first order, is just $f = P_{max}$. This algorithm, called **Jet Probability**, is interesting also for its ability to enrich the sample with charm-originated jets, if the probability cut is set at a larger value ($P_{max} = 0.05$ is generally found as a good operating point for that purpose). A useful application of Jet Probability is discussed in Sec. 5.3.

Identification of soft leptons in b-jets provides an independent tool for b-tagging. However, the combined effect of leptonic branching ratio and sub-optimal identification efficiency of leptons inside hadronic jets make this tool a less powerful one than those based on track impact parameter.

Finally, a recent development has been the application of **Neural Networks** (one can hardly live without them these days!) to the discrimination of b-quark jets, based on the combined analysis of several variables sensitive to the flavor content of the jet. Once optimized, Neural Networks become the most effective tool for high-efficiency b-tagging.

b-jets also pose a challenge for their energy measurement, since some of their peculiarities are liable to affect the calorimeter determination of P_T. It was already noted above that this is a quite important issue for precise determinations of the top quark mass, which –to first order– is linearly correlated to the energy of the emitted b-jet in the rest frame of top decay. Moreover, the resolution of the b-jet energy has already been described above as a critical parameter in determining the Tevatron discovery reach for a light Higgs boson.

A distinguishing feature of jets originated from b-quarks is that they show a harder fragmentation than light-quark and gluon jets: this represents a source of bias in the energy measured in calorimeters whose e/π response (the ratio of response to electrons and charged pions of equal incident energy) is non-linear with momentum, as is often the case. A second issue is the copious amount of semileptonic decay of B hadrons, which causes a negative average offset in the response through energetic neutrinos escaping the detector unmeasured and muons behaving as minimum-ionizing particles: this causes a scale offset and a degradation in resolution. Third, b-jets produced by electroweak processes may be color-disconnected from the initial state (not so in top quark decay, but rather in Z or H decay), with a resulting difference in soft gluon radiation and in the resulting structure of out-of-cone energy, again affecting the energy scale, as well as the resolution if one applies a scale correction for the out-of-cone energy tuned on light quark or gluon jets.

The main difficulty in handling the peculiarities discussed above is the lack of suitable datasets where to measure biases, test corrections, and derive improvements. As we discussed above, the jet response in the calorimeter is equalized using large samples of dijet events, and tested with sizable amounts of gamma-jet events. Neither of these techniques are viable for b-jets, although CDF data collected with SVT triggers will eventually enable some statistics-limited checks.

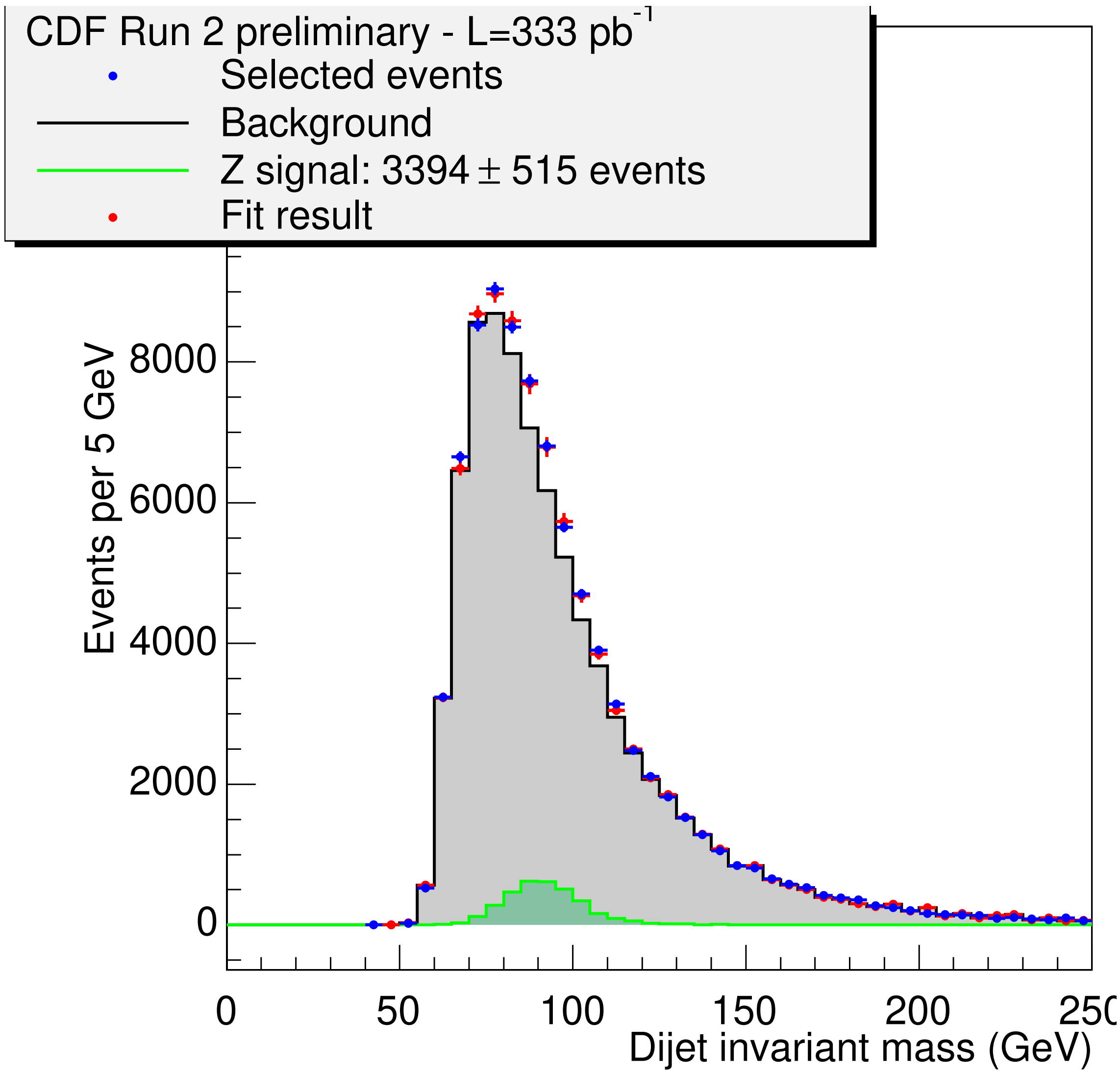

Figure 11. The signal of $Z \to b\bar{b}$ decays extracted from 333 pb^{-1} of CDF Run II data is visible as an excess of events in the dijet mass region around 90 GeV. The green histogram shows the fitted Z contribution.

The picture is not bleak, however, because the mentioned effects can be studied quite accurately with Monte Carlo simulations. The uncertainty in the b-quark fragmentation function is by now small enough that simulations should be able to determine the resulting bias in jet energy scale with satisfactory precision; the semileptonic decay is also well known; the details of color flow and soft gluon radiation are by now modeled well enough that a residual effect of their uncertainty on the jet energy scale should be minimal. All in all, these issues appear under control.

Furthermore, a large-statistics $Z \to b\bar{b}$ peak observed in CDF data collected by a dedicated SVT trigger can provide an independent sanity check and a reduction of systematic uncertainties on the b-jet energy scale. The signal has been extracted from $333pb^{-1}$ of Run II data (see Fig. 11), and the goal is now to measure the scale with 1% accuracy using at least $1fb^{-1}$ of data. Besides providing a precise measurement of the b-jet energy scale, the signal will also allow tests of algorithms devised to improve the b-jet energy resolution.

Another idea, recently investigated by DØ , is to determine the b-quark jet energy scale from photon-jet events where the heavy flavor content of the jet is enriched by b-tagging. Despite the small cross section of γb production, these events might allow to extract a meaningful measurement of the b-jet E_T scale by fitting the so-called missing-E_T projection fraction, defined by

$$MPF = 1 + \frac{\vec{E}_T^{miss} \cdot \vec{n}_T^{\gamma}}{E_T^{\gamma}},$$

where $\vec{E}_T^{miss}$ is the missing transverse energy in the event, $\vec{n}_T^{\gamma}$ is the versor of the photon in the transverse plane, and E_T^{γ} is the transverse energy of the photon. The method works well if the fraction f_b of fake vertex tags in the data is determined with precision. The extraction of f_b is performed by combined fits to the combined invariant mass of tracks coming from the secondary vertex and the transverse flight distance between primary and secondary vertex.

4. Searches for the Standard Model Higgs boson

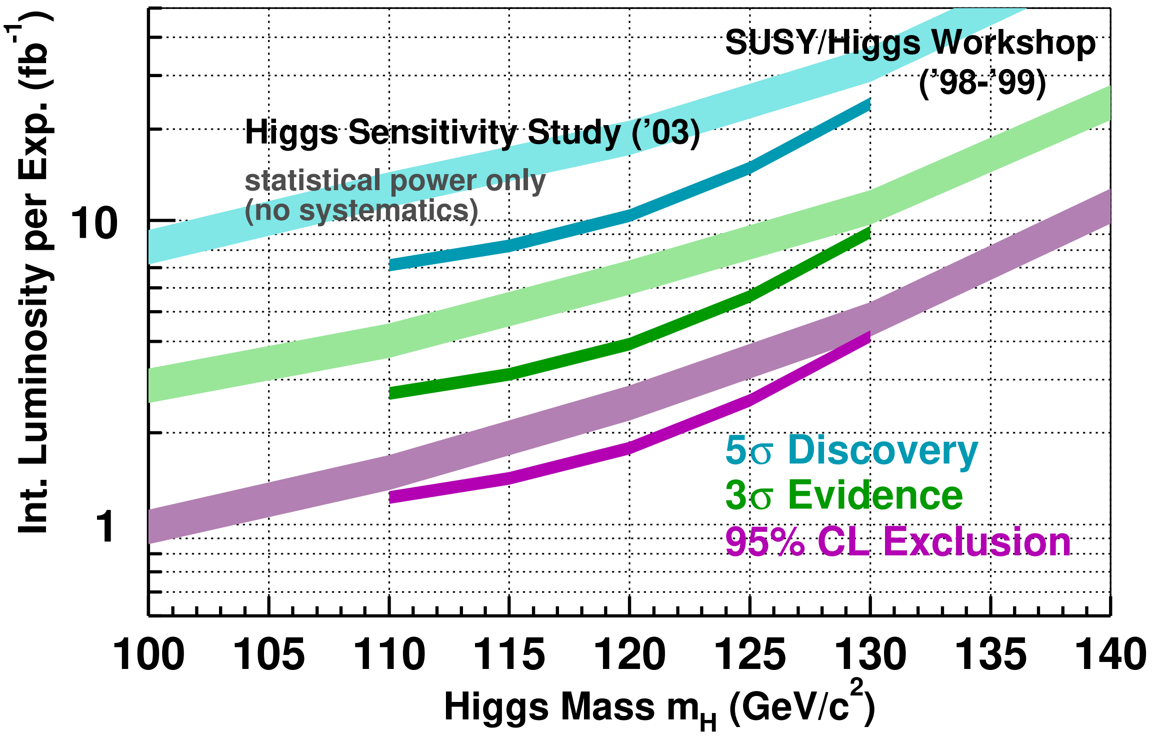

Figure 12. *The three pairs of bands show the integrated luminosity per experiment needed for a 95% exclusion (purple), a 3σ evidence (green), or a 5σ discovery (blue) of the Higgs boson as a function of the particle mass, obtained by the 1998 and 2003 studies. The 2003 study shows slightly reduced luminosity thresholds for any given mass, but does not include systematic uncertainties.*

The excellent agreement between experimental measurements of electroweak observables and Standard Model (SM) predictions constitute a strong motivation to search for the Higgs boson at the Tevatron [8]. The latest fits [9] –which indicate $M_H = 89^{+42}_{-30}$ GeV as the most likely value for the Higgs mass– together with the direct lower limit $M_H > 114$ GeV obtained by the LEP II experiments [10], allow CDF and DØ to hope for a significant measurement before the next big players at the LHC start collecting data.

In 2003, prompted by the US Department of Energy, a joint committee of CDF and DØ members carried out a reassessment of the Tevatron reach in the search for the Higgs boson [7]. By using a more realistic model of the two detectors than the simplified one used in a study performed in 1998 [11], and using real data collected by the experiments in the first years of Run II, the committee determined that the earlier claims of sensitivity were not off the mark: by searching in all significant decay channels, and combining CDF and DØ measurements together, the extrapolations obtained in 1998 were nicely confirmed (see Fig. 12). In the meantime, the Tevatron has continued to improve its performance, recently surpassing the peak luminosity of $1.8 \times 10^{32} cm^{-2} s^{-1}$. The chances of the Tevatron delivering an integrated statistics of $8fb^{-1}$ to each experiment by the end of 2009 appear now sizeable. Before the CMS and ATLAS collaborations start analyzing their first collisions, CDF and DØ might just be able to either discover a 115 GeV Higgs boson, or exclude it up to a mass of 135 GeV.

The search for the Higgs boson at the Tevatron is carried out by looking for two main decay channels, depending on the particle mass. For masses below 135 GeV, the dominant decay is $H \to b\bar{b}$, and the final state always includes the leptonic decay of an accompanying W or Z boson to allow triggering on the signal; the latest results from CDF and DØ in these final states are given in Sec. 4.1. For masses above the 135 GeV threshold, the $H \to WW$ decay provides the most promising signature. In that case, both direct production of Higgs bosons (yielding a WW final state) and associated production of a Higgs and an electroweak boson (yielding the spectacular signature of three vector bosons together) are considered; results are discussed in Sec. 4.2.

4.1. Light Higgs Boson Searches

Both CDF and DØ have analyzed their Run II datasets in search for associated production of a W or Z boson and a pair of b-quark jets from $H \to b\bar{b}$ decay, using the reconstructed dijet mass distribution as the prime tool to extract limits to the cross section times branching ratio of the process.

In $695pb^{-1}$ of collider data CDF finds 29 events with a clean $W \to l\nu$ ($l = e, \mu$) candidate and two jets both tagged by the secondary vertex identification algorithm described in Sec. 3.4; estimated standard model backgrounds amount to 32.2 ± 6.2 events (Fig. 13, left). From a fit of the dijet mass distribution of these events, and a similar fit to an orthogonal set of $W+2$ jet events which contain a single b-tag but are signal-enriched by a neural network, a 95% C.L. limit ranging from 4 to $2pb$ is obtained for Higgs boson masses from 110 to 150 GeV. Similar limits are obtained by DØ who has so far analyzed a smaller dataset for this particular analysis. DØ limits range from 2.8 to 3.1 pb for $M_H = 115$ to 145 GeV (see Fig. 13, right).

A peculiar signature can be observed when a light Higgs boson is produced in association with a Z boson, and the latter decays to a pair of neutrinos. One may then observe a pair of b-jets with significant missing transverse energy. CDF has searched for this signature using data triggered by the requirement of SVT tracks with significant impact parameter and missing E_T. In 289 pb^{-1} of data they find 19 candidates, when 19.7 ± 3.5 are expected from background processes (Fig. 14).

The DØ collaboration also looks for the same signature in $261pb^{-1}$ of data. They make separate searches for the Higgs boson in double b-tagged and single b-tagged data, by applying a search window in the dijet mass distribution, centered at the nominal value of M_H and with a width equal to three times the experimental dijet mass resolution. They always find good compatibility for the background-only hypothesis: for instance, for a $M_H = 115$ GeV search

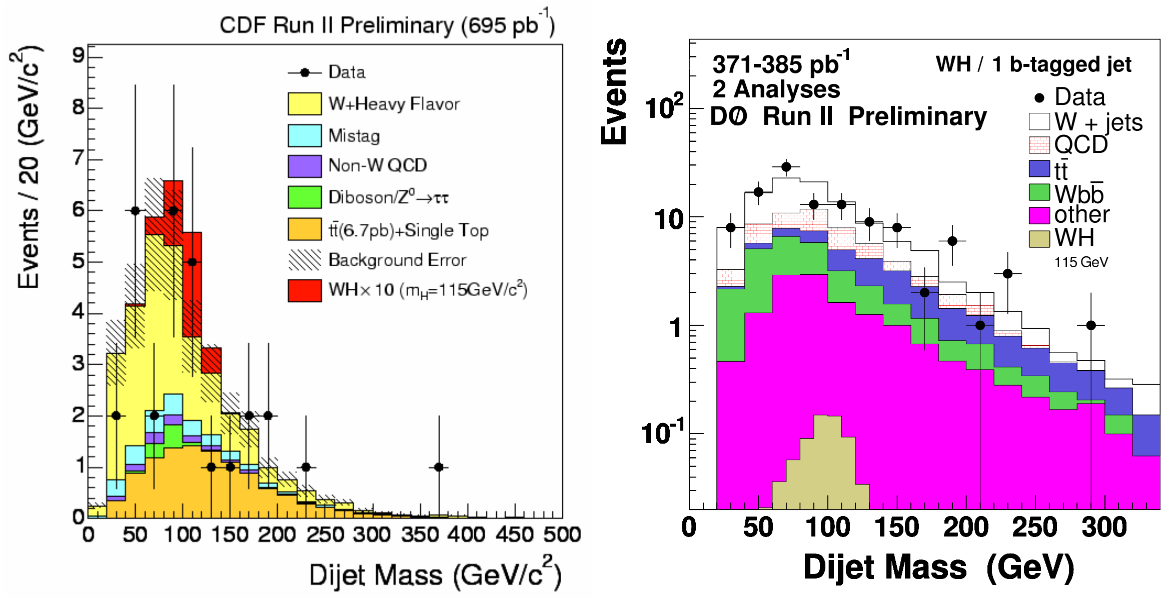

Figure 13. *The dijet mass distribution of 29 W +2 jet candidates (black points) is understood as a sum of several contributing SM backgrounds (left); a $H \to b\bar{b}$ signal 10 times larger than that expected by theoretical calculations is overlaid. Right: the dijet mass of doubly b-tagged W+ 2 jet candidates found by DØ is compared to the sum of expected backgrounds and to the expected signal contribution.*

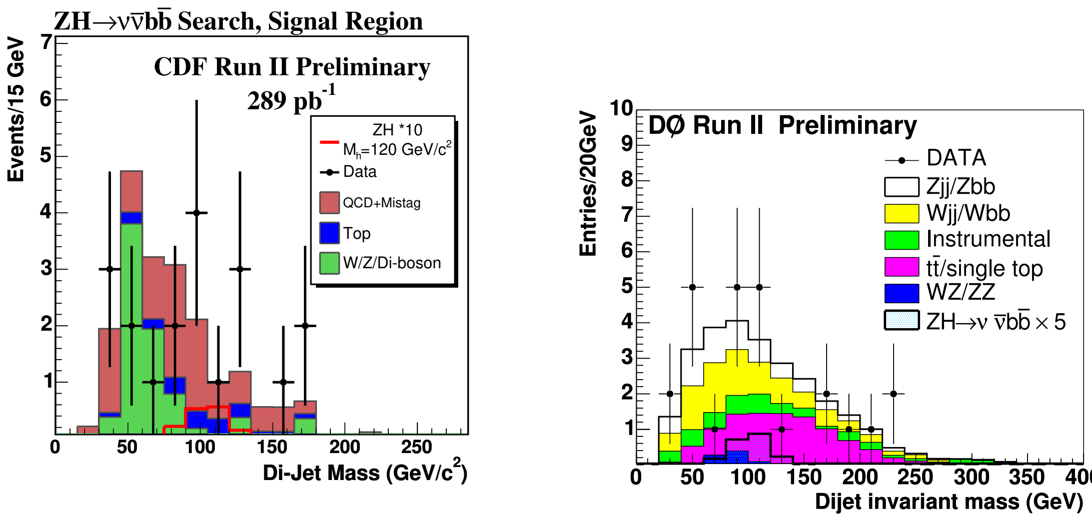

Figure 14. *The dijet mass distribution of double b-tagged $ZH \to \nu\nu b\bar{b}$ candidates from CDF (left) and DØ (right).*

they find 11 candidates in the double b-tagged data, with 9.4 ± 1.8 expected from background sources; and 33 single b-tag candidates with 34 ± 6.1 expected from background sources. The event counts are finally used to set limits from this channel at 3.5 to 2.4pb for M_H ranging from 105 to 135 GeV.

4.2. High Mass Searches

For any value of Higgs boson mass above 135 GeV the $H \rightarrow WW^{(*)}$ decay mode is the dominant one. When both W bosons decay to an electron-neutrino or muon-neutrino pair the final state is quite clean, with residual backgrounds mostly due to Drell-Yan production of lepton pairs. To discriminate direct production of a Higgs boson from non-resonant WW production - which in the standard model has a sizeable cross section [16] – it is useful to study the azimuthal angle $\Delta\Phi_{ll}$ between the two charged leptons, since the zero spin of the Higgs boson and helicity conservation conspire to produce leptons in the same direction in the transverse plane.

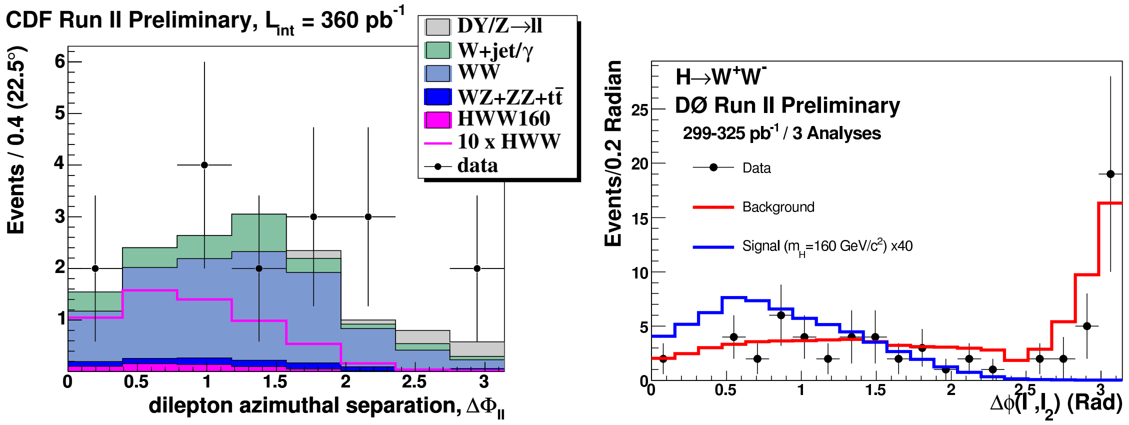

Figure 15. *Azimuthal angle between the two charged lepton candidates in the CDF (left) and DØ (right) $H \rightarrow WW$ analyses.*

CDF selects WW pairs by identifying lepton pairs of opposite charge, $P_T > 20$ GeV, and then applying a missing E_T cut at 25 GeV and a tight jet veto. A small dilepton mass is then required: $M_{ll} < 55$ (80) GeV for $M_H = 140$ (180) GeV. The resulting $\Delta\Phi_{ll}$ distribution is shown in Fig. 15 for the $360pb^{-1}$ of Run II data analyzed so far in this channel.

DØ has recently updated their own searches of the same final state by using $950pb^{-1}$ of Run II data. They require the azimuthal angle between the charged leptons to be $\Delta\Phi_{ll} < 2$ radians, and apply several additional cuts on kinematical quantities depending on the target Higgs boson mass. For the $M_H = 160$ GeV search they find 28 WW candidates, when 34.7 ± 1.7 are expected from non-Higgs SM sources. They thus obtain the limit of $\sigma_H \times B(H \rightarrow WW) < 2.2pb$ at 95% C.L. for $M_H = 160$ GeV.

CDF also searched $193.5pb^{-1}$ of data for the striking signature of associated WH production at high M_H, when the event may yield *three* W bosons. The search starts from a dataset of lepton pairs of the same charge, which is understood as a sum of fake lepton backgrounds and SM sources (see Fig. 15, right). Optimized cuts are then applied to the leptons transverse momentum and to the vector sum of lepton transverse momenta, $P_{T_{12}} > 35$ GeV. Zero events are observed, with 1.0 ± 0.6 expected from known sources. A 95% C.L. cross section times branching ratio limit of $8pb$ can thus be set for $M_H = 160$ GeV (see Fig. 16).

Figures 16 and 17 summarize the present status of Higgs boson searches at the Tevatron. It is necessary to note that most searches are still based on relatively small amounts of data; furthermore, CDF has not performed a combination of their results yet. The standard model prediction for Higgs production appears still far away: nevertheless, results are still roughly in line with those predicted by the 2003 Higgs sensitivity study, if one accounts for the statistics used by the analyses; moreover, several improvements in b-tagging efficiency and background rejection, as well as in the dijet mass resolution for pairs of b-jets, are under testing but still not used.

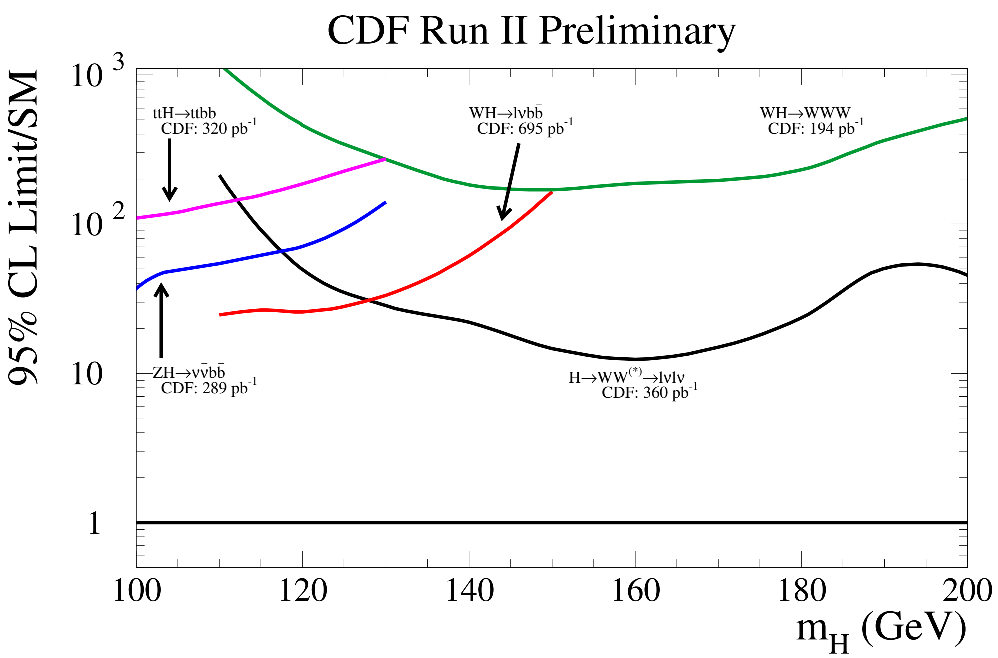

Figure 16. *Summary of 95% C.L. limits for Higgs boson production obtained by CDF in several search channels.*

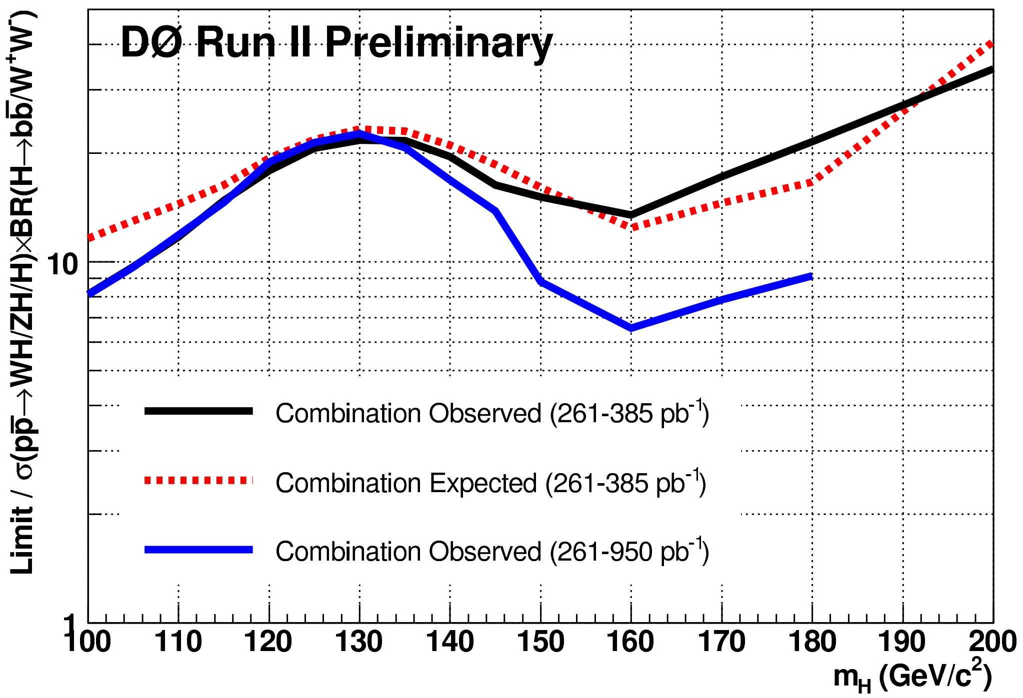

Figure 17. *Summary of 95% C.L. limits obtained by DØ from Run II searches of the Higgs boson. The y axis shows the ratio between determined limit and standard model cross section.*

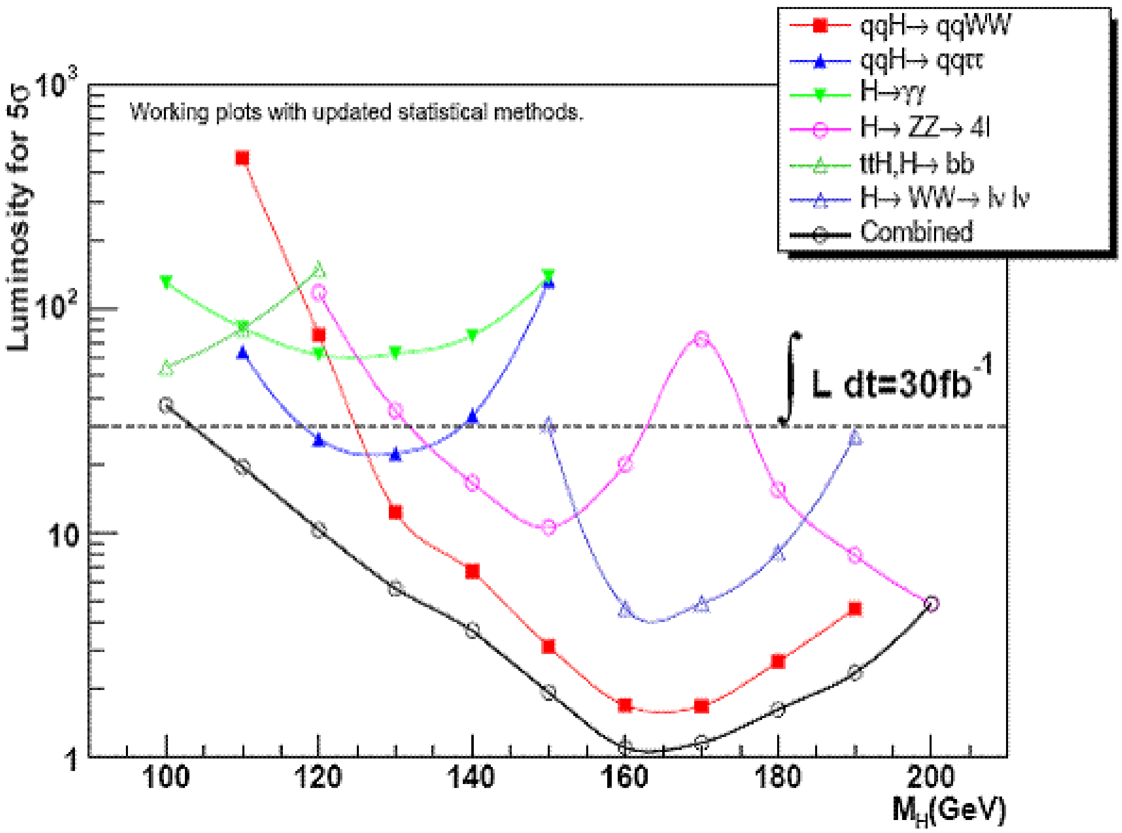

Figure 18. *Expected luminosity needed by the ATLAS detector to observe Higgs boson production as a function of the Higgs boson mass.*

The Higgs mass region below 130 GeV has been recently shown by the ATLAS and CMS experiments to be quite difficult to investigate with $\mathcal{O}$ $(10fb^{-1})$ of integrated luminosity (see *e.g.* Fig. 18 for recent ATLAS predictions). If –as appears probable given the prediction of electroweak fits and the recent world average of the top quark mass– the Higgs boson is indeed lighter than 130 GeV, a whole set of scenarios opens for year 2009, when LHC experiments will try to produce physics results with data from the first year of physics run, and CDF and DØ will squeeze the most out of their by then complete datasets.

The first scenario sees the Tevatron failing to deliver luminosity as described in the design plan (see Sec. 1.1): in that case, CMS and ATLAS will have no competitors in the search for the Higgs boson. The second scenario consist in a successful Tevatron running throughout year 2009, and a smooth start for the LHC experiments. In that case, a light Higgs boson might be observed on either side of the Atlantic ocean, and soon confirmed on the other side. The third scenario is the most favorable for the Tevatron, delivering luminosity according to the design plan while LHC further delays its startup date or experiences a bumpy start. In that case, CDF and DØ will have a significant chance of ending up as winners of the Higgs race, after all.

The forthcoming years will no doubt be extremely interesting and exciting for high P_T physics!

5. Top quark measurements

Ten years after the discovery of the top quark, the Tevatron experiments have started using $t\bar{t}$ events for precision measurements and as a laboratory for electroweak physics of quarks free from non-perturbative QCD effects.

The transition from the searches and then the first observations and measurements in Run I to the precision studies in Run II has been smooth, because the general strategy of the analyses has not changed: as more and more data is collected, cross section measurements are first performed; then determinations of the top mass follow, and studies of decay kinematics and searches for anomalies in production dynamics. Lastly, measurements of intrinsic physical properties are performed. The above *modus operandi* allows to optimize the output of physics results as analysis tools become more sophisticated and as the data are understood with increasing precision.

In the following is presented a summary of results on top cross section and top mass, and a mention of the most recent results of the search for single top production.

5.1. Brief introduction to top quark physics

At the Tevatron, production of $t\bar{t}$ pairs occurs by $q\bar{q}$ annihilation (85%) or gluon-gluon fusion (15%): proportions are exactly inverted from those that the LHC will provide. The next-to-next-to leading order prediction for top quark pair production cross section [15] is $6.1pb$: one $t\bar{t}$ event is produced every ten billion inelastic collisions. That translates into a rate of about two top events per hour in the interaction regions.

Electroweak-mediated single top production is not irrelevant, being half as frequent; its signature, however, is way less characteristic, such that so far CDF and DØ have been able to only obtain upper limits to that process. In the remainder of this section, only pair production is discussed.

Since $V_{tb} \sim 1$ and $M_t > M_W + M_b$, the top quark almost exclusively decays to a W boson and a b quark. Final states of $t\bar{t}$ pairs are classified according to the decay of the two produced W bosons: when both decay to an electron-neutrino or muon-neutrino pair, the *dilepton* mode arises; when one of the two W's decay to jet pairs and the other produces a $e\nu$ or $\mu\nu$ pair the final state is called *single lepton*; when both bosons decay to jet pairs, one has the *all-hadronic* final state. Decays to $\tau\nu$ pairs are excluded from this classification because of the less clear-cut signature of τ leptons, and because of the difficult identification of these particles: final states including τ leptons add a minor over-efficiency to analyses selecting the three final states mentioned above.

Top quark decays allow excellent studies of weak interactions of quarks, because of the large top quark mass. In fact, the top quark width –which is a cubic function of M_t– is computed to be $\Gamma_t \sim 1.5$ GeV, thus much larger than Λ_{QCD}. The top quark therefore is produced and decays free from non-perturbative QCD effects. Also, the top quark polarization can be measured in its decay, since the depolarization time $\tau_d = M_t/\Lambda^2_{QCD}$ is much longer than the decay time.

5.2. Production cross section measurements

The most precise $\sigma_{t\bar{t}}$ measurements come from the analysis of b-tagged single lepton decays, which represent a perfect compromise between signal to noise ratio and total yield.

The general recipe for selecting a signal-rich sample in the single lepton topology entails triggering on electrons or muons with $E_t > 15$ GeV or $P_t > 15$ GeV, respectively; offline, those thresholds are increased to 20 GeV, to which is added a requirement that the missing transverse energy $\not{E}_T$ detected by the calorimeter be $\not{E}_T > 25$ GeV (at CDF) or 30 GeV (at DØ). To extract the top signal from backgrounds, principally due to $W+$ jets production, events with a minimum of three hadronic jets are selected, and at least one jet is required to contain a secondary vertex b-tag.

Both CDF and DØ use Monte Carlo simulations to estimate physical backgrounds, while real data in suitable control regions depleted of $t\bar{t}$ contamination are employed to estimate the rate of false b-tags leaking in the signal samples. Events with only one or two jets besides the $W \to l\nu$ signature are used to verify sample composition and yield.

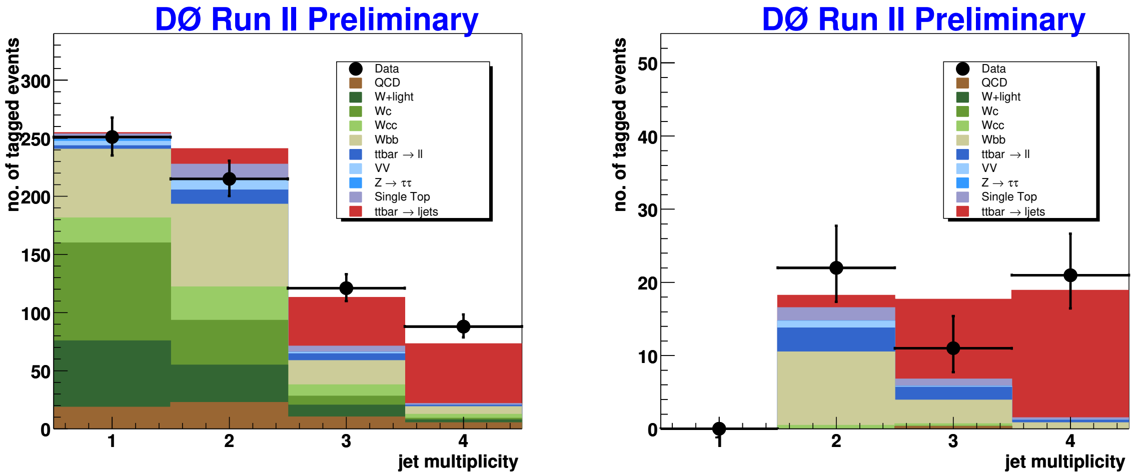

Figure 19. Distribution of the number of jets in selected W + jet events by the DØ collaboration. Left: single b-tags; right: double b-tags.

As an example, the standard single lepton analysis in DØ uses events with a triggering electron or muon, missing $E_t > 30$ GeV, three or four jets with $E_t > 20$ GeV, and one or two secondary vertex b-tags. The selected data is then divided into eight separate categories depending on their characteristics (e or μ, three or four jets, one or two b-tags) and the eight independent determinations are combined in a likelihood fit. The result is $\sigma_{t\bar{t}} = 8.1^{+1.3}_{-1.2} \pm 0.5_{lumi} pb$. Figure 19 shows the selected data and its composition in terms of the contributing processes.

Each experiment has by now produced about a dozen different measurements of the $t\bar{t}$ cross section. The various CDF determinations have been combined by properly taking into account common sources of systematic uncertainties such as integrated luminosity and b-tagging efficiency. The obtained average value has a comparable precision to theoretical estimates. The base data and the average are shown in Fig. 20.

5.3. Top mass determinations

The Tevatron experiments have put a big effort to measure the top quark mass with the highest possible precision. The top mass is a fundamental parameter of the standard model, and its precise determination constitutes a very stringent test of consistency of the theory. This can be stated quantitatively by observing that a 1 GeV uncertainty in the top quark mass has the same constraining power on the unknown mass of the Higgs boson as a 6.1 MeV uncertainty on the W boson mass [17].

Another compelling reason to measure the top quark mass with the utmost precision is the intriguing fact that its Yukawa coupling appears to be "natural": from the world average value of M_t one finds $y_t = \sqrt{2}\frac{M_t}{v} \sim 1.00$, with a precision of 1.3%. Many believe that the more we

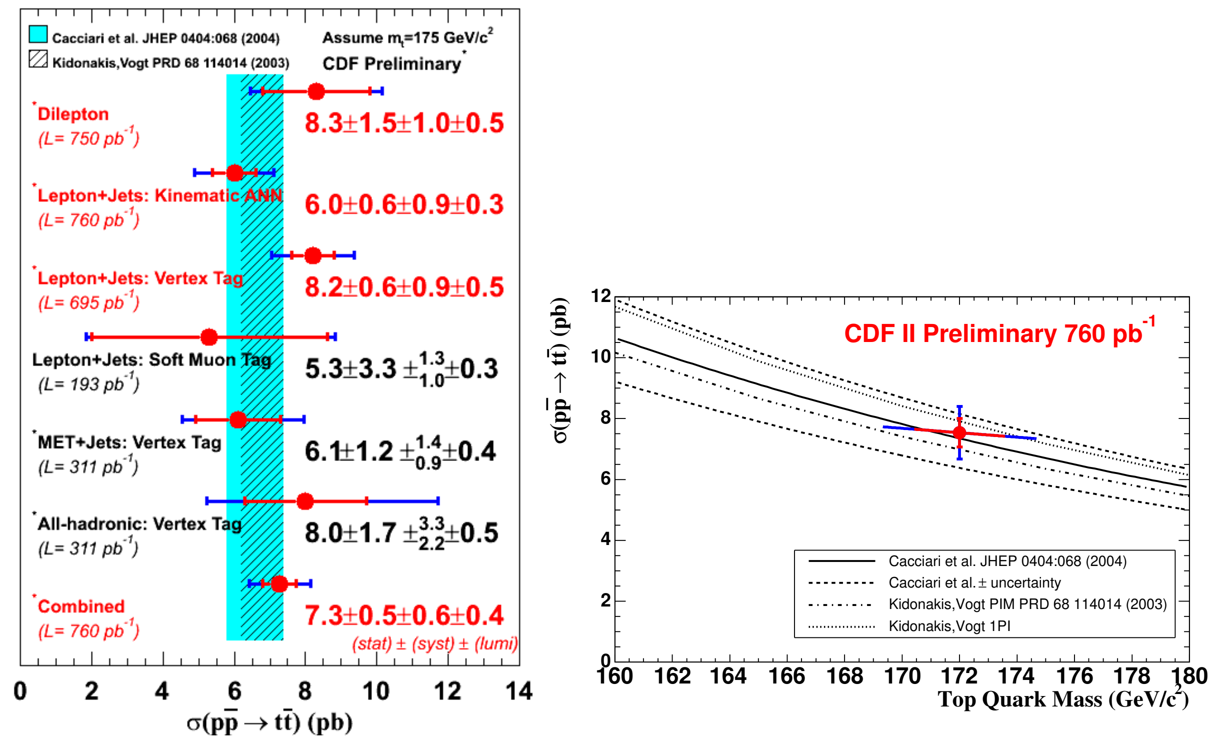

Figure 20. Left: summary of Run II measurements of the $t\bar{t}$ cross section by the CDF collaboration. Right: comparison of measured mass and top cross section with theoretical curves.

know about the top quark, the closest we will get to understanding the mechanism of electroweak symmetry breaking.
Several new methods have been devised to improve the precision of older measurements. In general, as collected statistics improves, the systematic uncertainty due to the knowledge of the jet energy scale (JES) becomes the target where to shoot all the bullets.

The jet energy scale has been determined with great precision by CDF using dijet events and gamma-jet events, as discussed in Sec. 3.1. However, the decay of top pairs offers an independent calibration point for jet energy through the knowledge of the W boson mass. The most precise single measurement of the top mass indeed comes from the use of that methodology. From a dataset of $680pb^{-1}$ of single lepton decays, with the selection of events containing four jets, a χ^2 technique finds the most probable value of the top mass by simultaneously fitting the JES from the $W \to q\bar{q}'$ portion of the hadronic decay. The result is $M_t = 173.4 \pm 1.7_{stat} \pm 1.8_{JES} \pm 1.3_{syst}$GeV (see Fig. 21). A measurement from DØ in the same channel, which also fits the jet energy scale together with the top quark mass, finds $M_t = 170.6 \pm 4.4_{stat+JES} \pm 1.7_{syst}$ GeV in a smaller sample of $380pb^{-1}$ of Run II data.

Interestingly, new methods have allowed the dilepton and all-hadronic channels to provide determinations of the top quark mass which have remained competitive with the precise single lepton measurements. In the dilepton channel CDF uses a matrix element technique based on finding for each event the posterior probability for the top mass as a product of the differential cross section for leading order $t\bar{t}$ production. In $750pb^{-1}$ of data the result is $M_t = 164.5 \pm 4.5 \pm 3.1$ GeV. In the all-hadronic final state a combination of matrix element and template fitting technique called *ideogram method* allows to extract $M_t = 177.1 \pm 4.9_{stat} \pm 4.7_{syst}$ GeV. The combined CDF average resulting from the above determinations is $M_t = 172.4 \pm 1.5_{stat} \pm 2.2_{syst}$

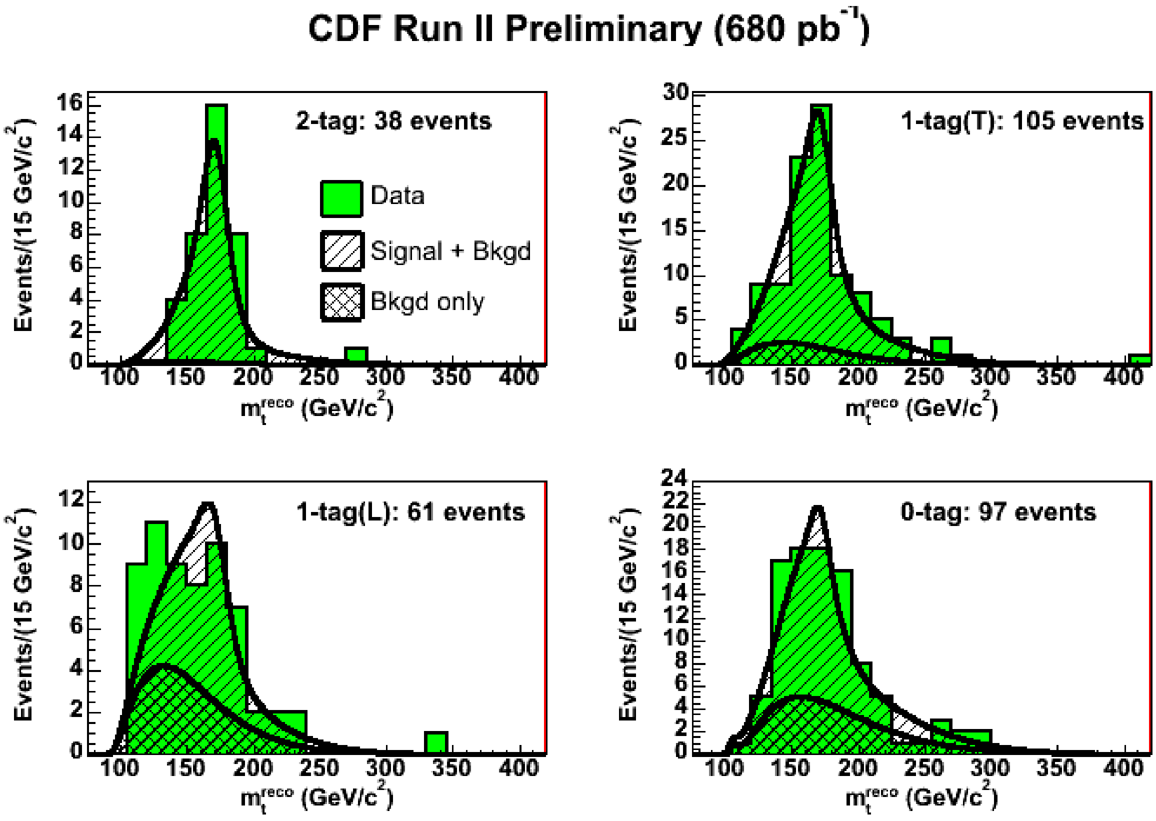

Figure 21. Reconstructed top mass from four independent subsets of single lepton $t\bar{t}$ candidates by CDF.

GeV.

Fig. 22 shows a summary of recent measurements of the top quark mass by CDF and DØ . A new world average has been computed recently by the Tevatron electroweak working group [18]: $M_t = 172.5 \pm 1.3_{stat} \pm 1.9_{syst}$ GeV. The uncertainty is now at 1.3%: by 2009, the Tevatron might be able offer a top quark mass with 1.2 GeV precision.

LHC will certainly benefit from a precise measurement of the top mass in its first phase, when M_t can be used as a calibration point for a first jet energy scale determination. However, the indirect information on the mass of the standard model Higgs boson extracted from electroweak fits using the Tevatron measurements of M_W and M_t will still be insufficient to provide a target Higgs mass to aim at. Until we find it, the Higgs boson will require us to carry out searches in all measurable final states.

5.4. Electroweak production of single top quarks

The electroweak process of single top production has not been observed yet by the Tevatron experiments. However, the 95% confidence level limits are by now quite close to the standard model expectations for the two main production mechanisms, W-gluon fusion and t-channel production via a virtual W boson (see Fig. 23). Theoretical predictions for the cross section of the two processes are of 1.98 and 0.88 pb, respectively [19, 20].

The observation of single top production would provide the only tool for measuring the Cabibbo-Kobajashi-Maskawa mixing matrix element V_{tb}, which is closely tied to the number of

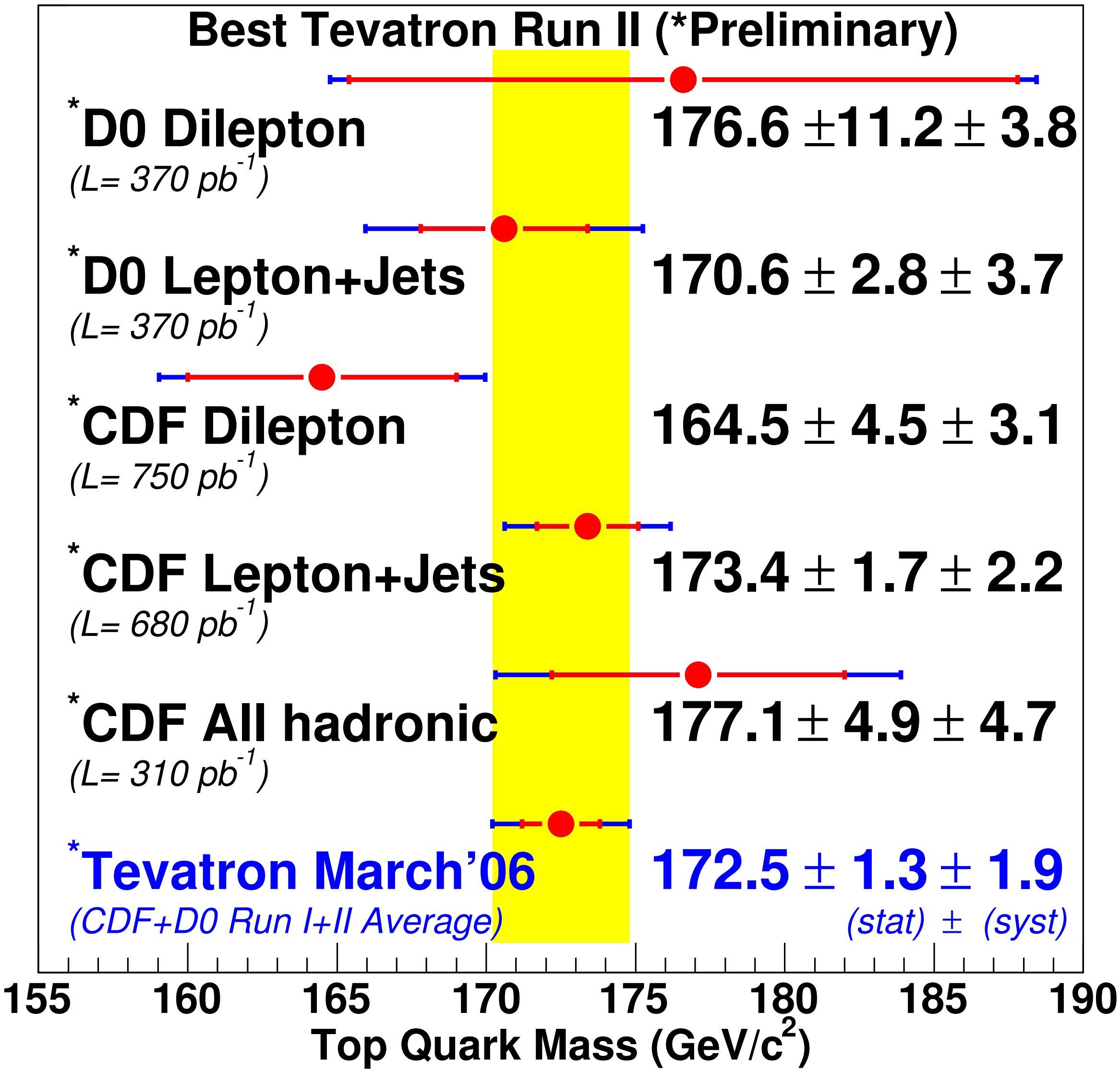

Figure 22. Summary of the best results on the top mass obtained in Run II by the CDF and DØ collaboration.

quark generations. Furthermore, the spin polarization of top quarks produced by the electroweak processes shown in Fig. 23 can be used to test the V-A structure of the weak charged current interaction. Of course, a precise measurement of these properties will only be accessible to the LHC experiments, and yet CDF and DØ have energetically attempted to find evidence for these processes in their Run II datasets, in the knowledge that measuring experimentally the production of single top at the Tevatron is important since it constitutes a background to light Higgs boson searches.

Currently, the best results come from CDF, who has recently completed the analysis of 700 pb^{-1} of data. The analysis is complex, and has been performed with two separate methods for the separation of signal and backgrounds based on the kinematical characteristics of the selected $W+$ 2 jet data: a neural network (whose output is shown in Fig. 24) and a multivariate likelihood. The

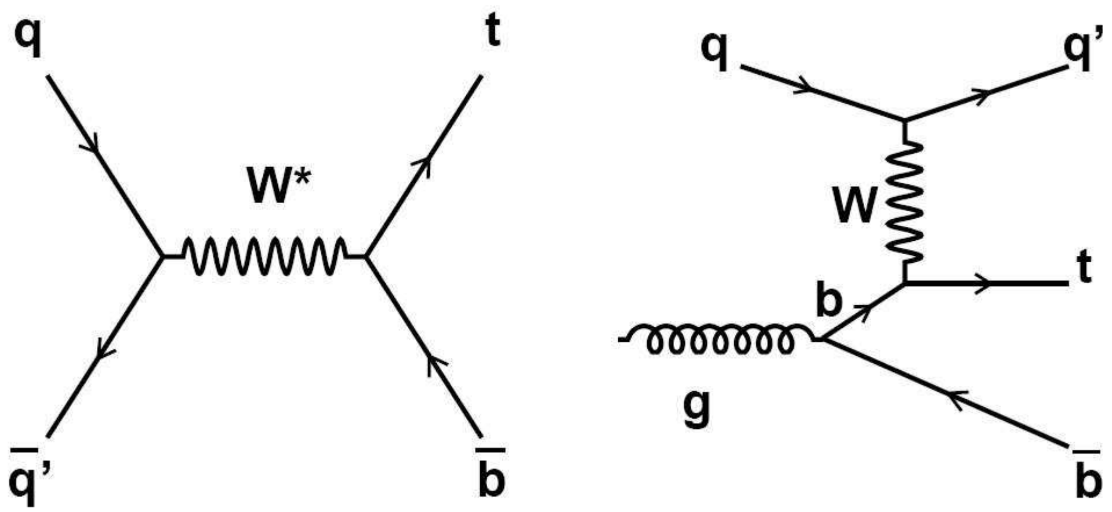

Figure 23. The two dominant diagrams for production of a single top quark at the Tevatron: s-channel off-shell W production (left) and W-gluon fusion (right).

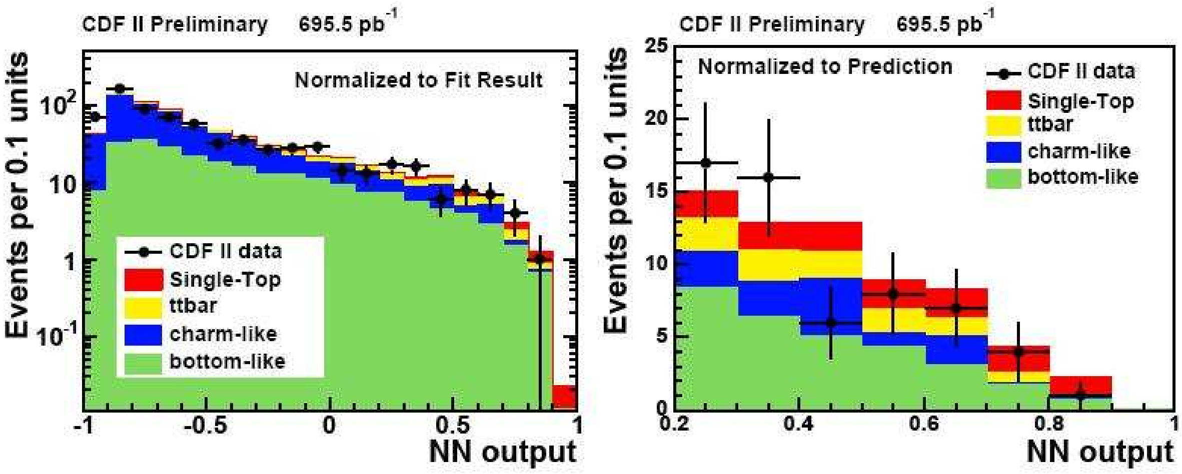

Figure 24. Results of the CDF search for single top production in 695 pb^{-1} of Run II data. On the left the entire output region of the neural network is shown, and the experimental data (black points) are compared to the sum of background processes and expected signal contribution (in red). On the right, a zoom into the signal region (NN output>0.2) is shown.

limit for the two production processes together is set at 3.4 pb at 95% C.L. by the neural network method, but I believe it is better to quote the most probable value for the signal cross section borne by the data, extracted by the multivariate likelihood: $\sigma_{s+t} = 0.8^{+1.3}_{-0.8}(stat)^{+0.2}_{-0.3}(syst)pb$.

6. Precision electroweak physics at the Tevatron

6.1. Vector boson production

If the million-event datasets of Z boson production at LEP made the headlines in the 1990's, the W and Z boson datasets currently collected at the Tevatron in Run II are no less impressive by now. Using the decays collected with high-P_T lepton triggers a lot of precision electroweak physics measurements can be performed, besides the mandatory W mass measurement. Inclusive and differential cross sections, limits on anomalous couplings and rare decays, cross sections for associated boson pair production are all physical quantities whose measurements are starting to be systematics-dominated. Fig. 25 and 26 show a few recent results obtained with Run II boson samples.

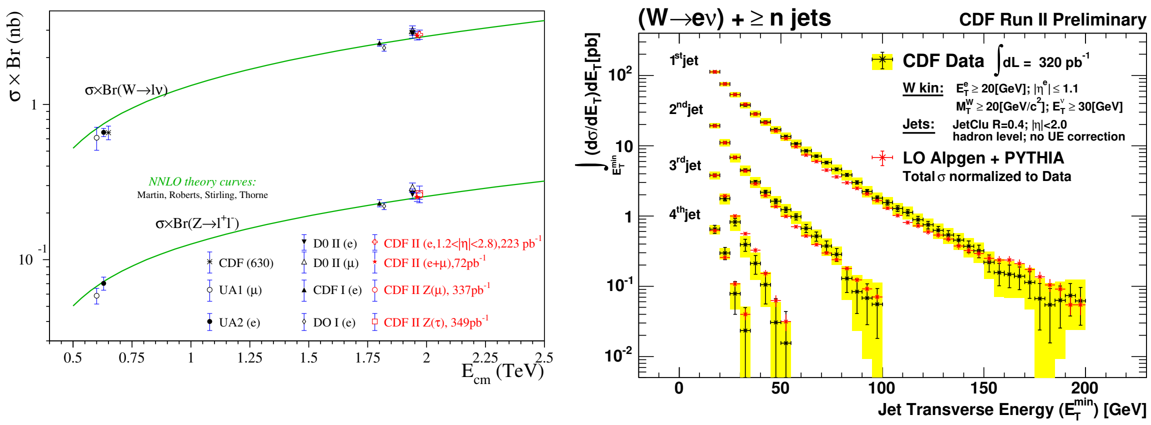

Figure 25. Left: summary of twenty years of W and Z boson cross section measurements at hadron colliders. Right: differential $W+$ jet cross section measurements by CDF as a function of jet E_t, for $N = 1, 2, 3, 4$ jets.

Here I will just mention the use of W decay to study the ratio of parton distribution functions $d(x)/u(x)$ in the proton, by measuring the charge asymmetry of the produced charged lepton. W bosons show in fact a production asymmetry at the Tevatron, due to the larger momentum carried by u quarks than d quarks in the proton. However, what is measurable is only the lepton rapidity, which obliges to $V - A$ coupling in W decay. It is worth noting here that at the LHC vector bosons will not exhibit any production asymmetry: this will prevent a *in situ* reduction of parton distribution functions (PDF) systematics in the measurement of the W mass.

CDF has pioneered the lepton charge asymmetry measurement in Run I, when the data helped constraining PDF fits at medium values of Bjorken's x, with the benefit of improving all subsequent W mass measurements by CDF and DØ . With Run II data, W decays are being studied in a wider rapidity range, thanks to the improved forward tracking of both detectors. Results (see Fig. 27) are putting the tightest constraints to the $d(x)$ and $u(x)$ distributions at medium values of x.

6.2. Parton Distribution Functions and cross section issues

An important contribution to LHC high-P_T physics measurements which the Tevatron experiments might offer is the improvement of the knowledge of proton PDF at very small values of x. Due to the very high center-of-mass energy, the precision of many cross section

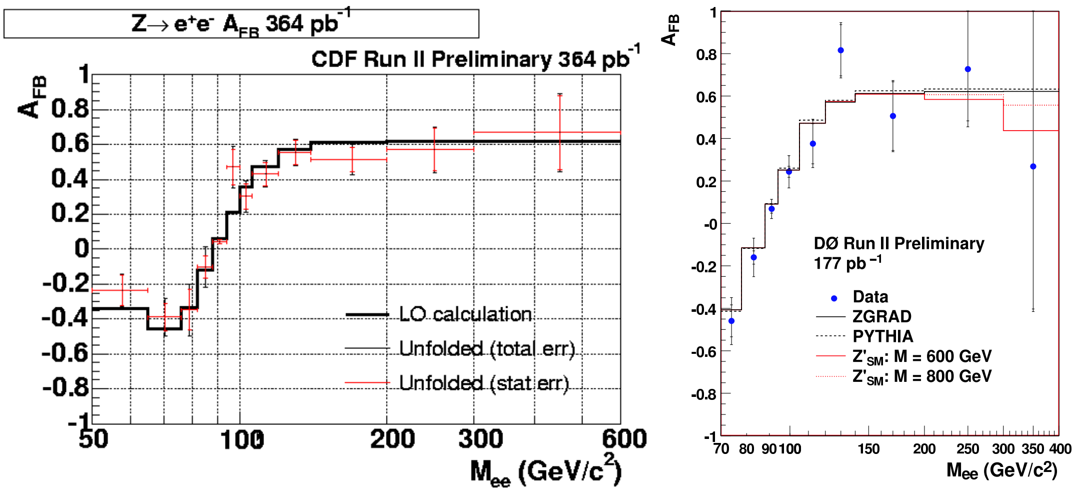

Figure 26. Tevatron results for the Drell-Yan production asymmetry as a function of the dilepton invariant mass. Left: The measurement by CDF. Right: measured Z asymmetry by DØ .

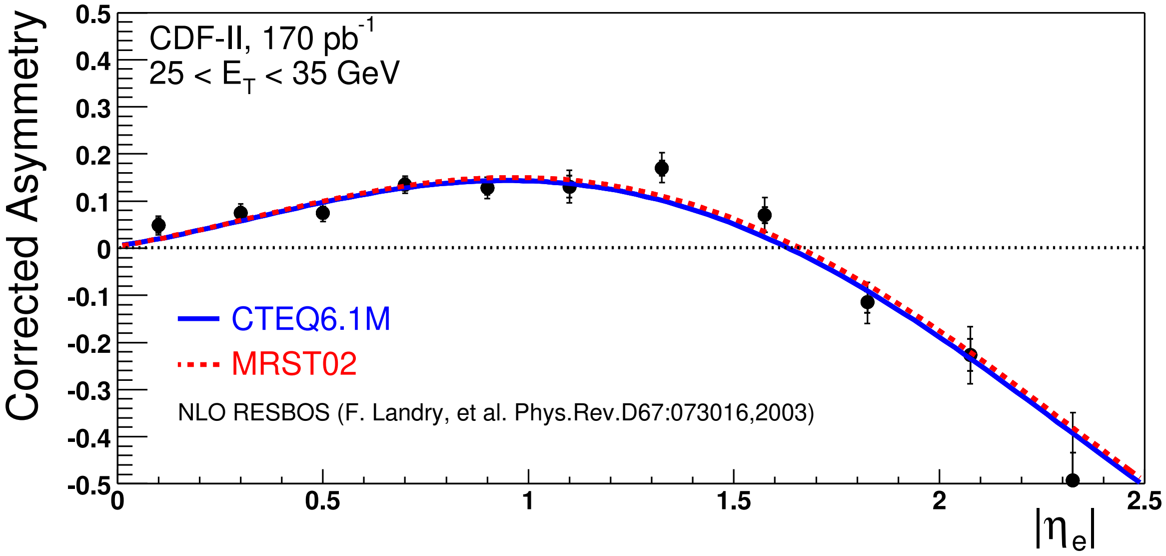

Figure 27. Lepton charge asymmetry in W decay measured by CDF as a function of lepton rapidity, for the bin of 25 to 35 GeV of lepton transverse energy. The data (points with error bars) are compared to two PDF sets.

measurements by the CMS and ATLAS collaborations will be limited by PDF systematics. The measurement of the W boson mass –for which the LHC goal is an accuracy of 15 MeV– will also strongly depend on the knowledge of production mechanisms for $x \simeq 5\times10^{-4}\div10^{-2}$. Other LHC measurements which could be critically affected by limited precision on small-x PDF include the top quark mass, and any counting experiment attempting to put in evidence a small excess due to a new physics signal, since these would rely on accurate predictions for background rates.

In absence of improvements from the Tevatron, LHC will heavily rely on data from the HERA determinations. But CDF and DØ *can* help. Measuring small-x PDF at the Tevatron requires the study of light things produced forwards. An attempt has already been done by DØ who have measured high-rapidity quarkonium production. Their measurement is still affected by insufficient statistics to provide a real constraint, but it certainly goes in the right direction, and it can only be hoped that both CDF and DØ will provide a precise determination with their full datasets in a few years.

Another interesting idea for the improvement of LHC cross section determinations has been supported by a recent paper [21]. All cross section measurements at the Tevatron – and the more so at the LHC – are affected by the knowledge of the inelastic cross section, which is known with a 4% precision. On the other hand, electroweak processes such as W production are now calculated to next-to-next-to leading order. One might then think of using the latter as a normailzation point of integrated luminosity for a given dataset.

By examining existing data from CDF and DØ one might draw the conclusion that it is indeed possible to measure $\sigma(W)$ to within $1-2\%$ both at the Tevatron and at the LHC. Again, the knowledge of parton distribution functions at high rapidity is critical. Another difficult problem is the need to know the stability of data taking conditions very accurately, and to model with precision the collection efficiency for high-P_T leptons. This can be done with the data itself: Z bosons have provided measurements of lepton ID efficiencies during the last 20 years. However, at present this remains a clever but as of yet untested method.

7. Conclusions

The CMS and ATLAS experiments, currently in construction at the Large Hadron Collider, will start producing physics results in 2009. By that date, the CDF and DØ experiments will be squeezing the most out of the several inverse femtobarns of proton-antiproton collisions collected since 2001: their analyses will represent both a challenge and a support to LHC precision measurements in the following years.

One challenge for LHC will be to improve measurements such as those of W and top quark masses, which will have reached already a high level of precision. A second challenge is of course constituted by the search for a light Higgs boson, where paradoxically $8fb^{-1}$ of pp collisions could prove insufficient for a discovery by CMS or ATLAS, whereas the same luminosity collected at a seven times smaller center-of-mass energy might be just enough for CDF and DØ .

But the Tevatron data will be an asset as well. LHC cross section measurements might strongly benefit from improved precision in the knowledge of parton distribution functions at small x, which can and should be provided by specific measurements by CDF and DØ . Further, the methodologies to improve the measurement of hadronic jets now under test at the Tevatron (in some instances –such is the case of the $Z \to b\bar{b}$ signal– on samples much harder to collect at 14 TeV) will be imported with confidence to the higher energy environment.

The perception in those sitting at the boundary between particle physics and funding agencies appears that CMS and ATLAS will only be successful if they discover new physics beyond the Standard Model. Some even believe that in the absence of anything new high energy physics might face the cancellation of all planned future projects [22]. I believe it is of paramount importance to demonstrate that LHC experiments can provide a huge advance in the knowledge of particle physics even if nothing is there to be found in going from 2 to 14 TeV besides a standard model Higgs boson: knowing with certainty that no new physics is manifest at the TeV scale is almost as much interesting, even if not as spectacular, as complex spectra of supersymmetric particles. That is the gamble that high-energy particle physics is facing in the next few years.

Acknowledgments
I wish to thank Riqie Arneberg for her editorial advice.

References

[1] S.Nagaitsev *et al.*, Phys. Rev. Lett. **96**, 044801 (2006).

[2] H.T.Shapiro *et al.*, *Revealing the Hidden Nature of Space and Time: Charting the Course for Elementary Particle Physics*, http://www7.nationalacademies.org/bpa/EPP2010.html .

[3] T.LeCompte and H.T.Diehl, *The CDF and DØ upgrades for Run II*, Ann. Rev. Nucl. Part. Sci. 50 (2000), 71.

[4] J.Huth *et al.*, *Research Directions for the decade*, Proceedings of the summer study on High energy Physics, Snowmass, Colorado, 1990, ed. E.L.Berger (World Scientific,1991).

[5] A.Bhatti *et al.*, *Determination of the Jet Energy Scale at the collider detector at Fermilab*, hep-ex/0510047 (2005).

[6] The jet energy correction method used by DØ in Run II has not been been published yet. Details can be found in http://www-d0.fnal.gov/phys_id/jes/public/plots_v7.1/index.html .

[7] CDF and DØ collaborations, *Results of the Tevatron Higgs Sensitivity Study*, FERMILAB-PUB-03/320-E.

[8] J.Gunion *et al.*, *The Higgs Hunter's Guide*, Addison-Wesley, New York 1990.

[9] The LEP Electroweak Working Group, http://lepewwg.web.cern.ch/LEPWWG/.

[10] A.Heister *et al.*, Phys. Lett. B **565**, 61 (2003).

[11] M.Carena *et al.*, *Higgs Working Group Report*, hep-ph/0010338.

[12] D.Acosta *et al.*, Phys. Rev. Lett. **94**, 091803 (2005).

[13] V.Abazov *et al.*, Phys. Rev. Lett. **94**, 151801 (2005).

[14] A.Bardi *et al.*, Nucl. Instr. Meth. A **409**, 658 (1998).

[15] N.Kidonakis and R.Vogt, Phys. Rev. **D68** (2003) 114014.

[16] The latest measurement by CDF is $\sigma_{WW} = 13.6 \pm 2.8_{stat.} \pm 1.6_{syst.} \pm 1.2_{lum.}$, see hep-ex/0605066.

[17] M.Beneke *et al.*, *Top Quark Physics*, hep-ph/0003033.

[18] Tevatron Electroweak Working Group, *Combination of CDF and DØ Results on the Mass of the Top Quark*, hep-ex/0603039.

[19] B.W.Harris *et al.*, Phys. Rev. **D66** (2002) 054024.

[20] Z.Sullivan, Phys. Rev. **D70** (2004) 114012.

[21] S.Frixione and M.Mangano, *How accurately can we measure the W cross section?*, hep-ph/0405130 (2004).

[22] A discussion on this topic has been hosted in P.Woit's web-log *Not Even Wrong*, see http://www.math.columbia.edu/~woit/wordpress/?p=399.